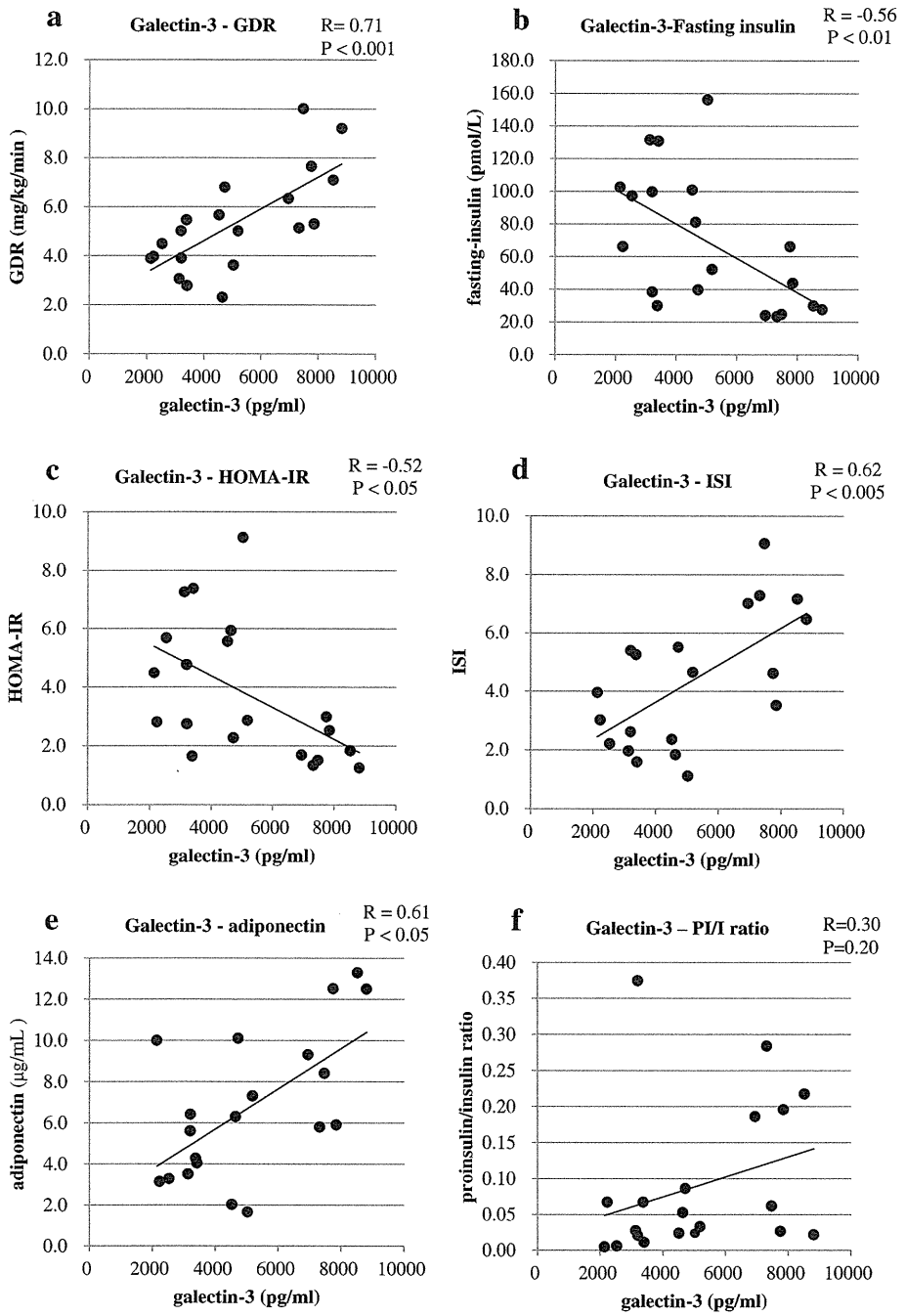

Figure 2 Correlation between galectin-3 and other parameters. Correlations between galectin-3 and GDR **(a)**, fasting insulin **(b)**, HOMA-IR **(c)**, ISI **(d)**, adiponectin **(e)**, and proinsulin/insulin (PI/I) ratio **(f)** were calculated by simple regression analysis.

of galectin-3 and adiponectin are low in type 2 diabetes patients with insulin resistance, indicating that the combination of low galectin-3 and adiponectin induce strong insulin resistance.

An animal study reported that CRP and IL-6 were significantly increased in the sera of galectin-3 deficient mice given a high-fat diet, whereas the levels of IL-10 were significantly decreased compared with the diet-matched wild type mice [8]. In our study, hs-CRP, IL-6 and IL-10 were not correlated with galectin-3. IL-10 has a protective role in type 2 diabetes by increasing insulin sensitivity in skeletal muscle [23]. We presumed that low levels of plasma galectin-3 and IL-10 reflect insulin sensitivity in skeletal muscle, because the glucose clamp technique mainly reflects insulin sensitivity in skeletal muscle. However, there was no correlation between IL-10 and

Table 3 Multiple regression analysis to examine an influencing factor of the galectin-3

$R^2 = 0.767$ R = 0.876	Partial regression coefficients	Standard partial regression coefficients	P value
Age	0.329	0.055	0.93
Gender	−0.007	0.503	0.38
BMI	−1.667	0.723	0.17
Waist circumference	−0.2481	−0.871	0.05
FPG	0.125	−0.829	0.08
HbA1c	−0.102	0.080	0.89
Fasting insulin	−0.564	−0.837	0.07
HOMA-IR	0.023	−0.098	0.337
Insulinogenic Index	0.402	−0.066	0.480
GDR	0.713	0.898	0.03
hs-CRP	−0.257	0.355	0.55
IL-6	−0.075	−0.196	0.75
IL-10	−0.146	0.274	0.65
Proinsulin/insulin ratio	0.297	0.833	0.08
adiponectin	0.614	−0.394	0.51
TG	−0.110	−0.266	0.66

The independent variables were: age, gender, BMI, waist circumference, FPG, HbA1c, fasting insulin, HOMA-IR, Insulinogenic Index, GDR, hs-CRP, IL-6, IL-10, proinsulin/insulin ratio, adiponectin, and TG. The significant standard partial regression coefficient was GDR 0.898 ($P < 0.05$).
BMI, body mass index; FPG, fasting plasma glucose; HOMA-IR, homeostasis model assessment of insulin resistance; GDR, glucose disposal rate; hs-CRP, high-sensitive C reactive protein; IL, interleukin; TG, triglyceride.

galectin-3 levels in this study. Further investigations are needed because the pathophysiology of type 2 diabetes patients may be different from that of galectin-3 knock-out mice. We consider that galectin-3 is associated with adiponectin rather than inflammation in patients with type 2 diabetes.

In our study, galectin-3 had a weak tendency towards negative correlation with the insulinogenic index, and a positive correlation with the proinsulin/insulin ratio. The proinsulin/insulin ratio is a marker of beta cell stress [12]. Galectin-3−/− mice were relatively resistant to diabetogenesis as evaluated by glycemia, quantitative histology and insulin content in streptozotocin induced diabetes [4]. These results imply that low levels of serum galectin-3 induce insulin resistance and hyperinsulinemia, but also may protect beta cell function. However, galectin-3 over-expression protected beta-cells from the cytotoxic effect of IL-1beta [6]. Moreover, young (12-week-old) galectin-3 deficient mice fed a standard diet exhibited altered glucose homeostasis in the absence of obesity and associated abnormalities [7]. Thus suggesting a direct positive modulation of beta-cell function by galectin-3 independent of obesity-related inflammation. In this study, there was no significant association, because one patient with low galectin-3 showed high PI/I ratio. The small number of our study has limitations, further investigations are needed. As the multiple regression analysis shows, we consider that galectin-3 is associated with insulin resistance rather than insulin secretion in patients with type 2 diabetes.

Galectin-3 is also one of the pattern recognition receptors that bind and mediate the degradation of modified lipoproteins and advanced glycation end products (AGE) [24]. In contrast to other receptors for AGE, galectin-3 protects from AGE-induced tissue injury. Therefore, galectin-3 ablation accelerates AGE-induced atherogenesis [25]. These results suggest that low levels of serum galectin-3 also induce atherosclerosis, and therefore, galectin-3 is an important molecule in type 2 diabetes.

Our study has several limitations, including the small number of patients and the variable nature of the medications for diabetes used by the study participants. Thus, our results require confirmation by a larger study. It is possible that the different medications used by the subjects modified the insulin responses in the MTT. For instance, metformin has been associated with lower systemic galectin-3 [3]. In our study, three patients were treated with metformin, which could have affected galectin-3 levels. A control group of insulin resistant non-diabetic subjects would be helpful in this regard, we are investigating a control group of insulin resistant non-diabetic subjects now. Despite these limitations, we consider that our study contributes to better understanding of the pathophysiology of type 2 diabetes.

Conclusion

Our results suggest that low levels of serum galectin-3 are associated with insulin resistance in patients with type 2 diabetes.

Abbreviations

AUC: Area under the curve; AGE: Advanced glycation end product; ELISA: Enzyme-linked immunosorbent assay; FPG: Fasting plasma glucose; GDR: Glucose disposal rate; GIR: Glucose infusion rate; HOMA-IR: Homeostasis model assessment for insulin resistance; hs-CRP: high-sensitive C-reactive protein; IL: Interleukin; IRI: Immunoreactive insulin; ISI: Insulin sensitivity index; JDS: Japan Diabetes Society; MTT: Meal tolerance test.

Competing interests

The authors declare that they have no competing interests.

Authors' contributions

TO wrote the manuscript and researched data. YF, RN, HS, KS, NY, KM, SI, HO and EU researched data. MK, EM, ST, and KY contributed to discussion and reviewed/edited manuscript. All authors read and approved the final manuscript.

Acknowledgments

This study was supported by the Japan Diabetes Foundation (2013), grants for young researchers from the Japan Association for Diabetes Education and Care (2013), Tottori University Faculty of Medicine Research Grant (2013) and Tottori University Hospital Research Grant (2012, 2013). We thank Ms.

Haruka Okada, Ms. Yoshiko Oda, and Ms. Maki Kameda for her excellent technical assistance. This work was carried out at Tottori University Faculty of Medicine, Tottori, Japan.

Author details
[1]Division of Cardiovascular Medicine, Endocrinology and Metabolism, Department of Molecular Medicine and Therapeutics, Tottori University Faculty of Medicine, Yonago, Tottori, Japan. [2]Department of Regional Medicine, Tottori University Faculty of Medicine, Yonago, Tottori, Japan. [3]School of Health Science, Tottori University Faculty of Medicine, Yonago, Japan. [4]Department of Molecular Biochemistry and Clinical Investigation, Osaka University Graduate School of Medicine, Suita, Japan.

Received: 12 July 2014 Accepted: 22 September 2014
Published: 27 September 2014

References

1. Yang RY, Rabinovich GA, Liu FT: **Galectins: Structure, function and therapeutic potential.** *Expert Rev Mol Med* 2008, **13**:e17–e39.
2. de Boer RA, Lok DJ, Jaarsma T, van der Meer P, Voors AA, Hillege HL, van Veldhuisen DJ: **Predictive value of plasma galectin-3 levels in heart failure with reduced and preserved ejection fraction.** *Ann Med* 2011, **43**:60–68.
3. Weigert J, Neumeier M, Wanninger J, Bauer S, Farkas S, Scherer MN, Schnitzbauer A, Schäffler A, Aslanidis C, Schölmerich J, Buechler C: **Serum galectin-3 is elevated in obesity and negatively correlates with glycosylated hemoglobin in type 2 diabetes.** *J Clin Endocrinol Metab* 2010, **95**:1404–1411.
4. Mensah-Brown EP, Al Rabesi Z, Shahin A, Al Shamsi M, Arsenijevic N, Hsu DK, Liu FT, Lukic ML: **Targeted disruption of the galectin-3 gene results in decreased susceptibility to multiple low dose streptozotocin-induced diabetes in mice.** *Clin Immunol* 2009, **130**:83–88.
5. Saksida T, Nikolic I, Vujicic M, Nilsson UJ, Leffler H, Lukic ML, Stojanovic I, Stosic-Grujicic S: **Galectin-3 deficiency protects pancreatic islet cells from cytokine-triggered apoptosis in vitro.** *J Cell Physiol* 2013, **228**:1568–1576.
6. Karlsen AE, Størling ZM, Sparre T, Larsen MR, Mahmood A, Størling J, Roepstorff P, Wrzesinski K, Larsen PM, Fey S, Nielsen K, Heding P, Ricordi C, Johannesen J, Kristiansen OP, Christensen UB, Kockum I, Luthman H, Nerup J, Pociot F: **Immune-mediated beta-cell destruction in vitro and in vivo-A pivotal role for galectin-3.** *Biochem Biophys Res Commun* 2006, **344**:406–415.
7. Pang J, Rhodes DH, Pini M, Akasheh RT, Castellanos KJ, Cabay RJ, Cooper D, Perretti M, Fantuzzi G: **Increased adiposity, dysregulated glucose metabolism and systemic inflammation in Galectin-3 KO mice.** *PLoS One* 2013, **8**:e57915.
8. Pejnovic N, Pantic J, Jovanovic I, Radosavljevic G, Milovanovic M, Nikolic I, Zdravkovic NS, Djukic AL, Arsenijevic NN, Lukic ML: **Galectin-3 deficiency accelerates high-fat diet induced obesity and amplifies inflammation in adipose tissue and pancreatic islets.** *Diabetes* 2013, **62**:1932–1944.
9. Kuzuya T, Nakagawa S, Satoh J, Kanazawa Y, Iwamoto Y, Kobayashi M, Nanjo K, Sasaki A, Seino Y, Ito C, Shima K, Nonaka K, Kadowaki T: **Committee of the Japan Diabetes Society on the diagnostic criteria of diabetes mellitus: Report of the Committee on the classification and diagnostic criteria of diabetes mellitus.** *Diabetes Res Clin Pract* 2002, **55**:65–85.
10. Yoshino G, Tominaga M, Hirano T, Shiba T, Kashiwagi A, Tanaka A, Tada N, Onuma T, Egusa G, Kuwashima M, Sanke T, Oikawa S, Honda K, Tachikawa T: **The test meal A:A pilot model for the international standard of test meal for an assessment of both postprandial hyperglycemia and hyperlipidemia.** *J Jpn Diabetes Soc* 2006, **49**:361–371.
11. Sumi K, Ohkura T, Yamamoto N, Fujioka Y, Matsuzawa K, Izawa S, Shiochi H, Kinoshita H, Ohkura H, Kato M, Yamamoto K, Taniguchi SI: **Long-term miglitol administration suppresses postprandial glucose-dependent insulinotropic polypeptide secretion.** *Diabetol Int* 2013, **4**:190–196.
12. Ohkura T, Inoue K, Fujioka Y, Nakanishi R, Shiochi H, Sumi K, Yamamoto N, Matsuzawa K, Izawa S, Ohkura H, Kato M, Yamamoto K, Taniguchi SI: **The proinsulin/insulin (PI/I) ratio is reduced by postprandial targeting therapy in type 2 diabetes mellitus: a small-scale clinical study.** *BMC Res Notes* 2013, **6**:453.
13. Kashiwagi A, Kasuga M, Araki E, Oka Y, Hanafusa T, Ito H, Tominaga M, Oikawa S, Noda M, Kawamura T, Sanke T, Namba M, Hashiramoto M, Sasahara T, Nishio Y, Kuwa K, Ueki K, Takei I, Umemoto M, Murakami M, Yamakado M, Yatomi Y, Ohashi H: **Committee on the Standardization of Diabetes Mellitus-Related Laboratory Testing of Japan Diabetes Society, "International clinical harmonization of glycated hemoglobin in Japan: From Japan Diabetes Society to National Glycohemoglobin Standardization Program values.** *J Diabetes Invest* 2012, **3**:39–40.
14. *National Institutes of Diabetes and Digestive and Kidney Diseases, the HbA1c converter, [article online].* 1999. Available from http://www.ngsp.org/convert1.asp.
15. DeFronzo RA, Tobin JD, Andres R: **Glucose clamp technique: a method for quantifying insulin secretion and resistance.** *Am J Physiol* 1979, **237**:214–223.
16. Kawamori R, Matsuhisa M, Kinoshita J, Mochizuki K, Niwa M, Arisaka T, Ikeda M, Kubota M, Wada M, Kanda T, Ikebuchi M, Tohdo R, Yamasaki Y: **Pioglitazone enhances splanchnic glucose uptake as well as peripheral glucose uptake in non-insulin-dependent diabetes mellitus. AD-4833 Clamp-OGL Study Group.** *Diabetes Res Clin Pract* 1998, **41**:35–43.
17. Tamura Y, Tanaka Y, Sato F, Choi JB, Watada H, Niwa M, Kinoshita J, Ooka A, Kumashiro N, Igarashi Y, Kyogoku S, Maehara T, Kawasumi M, Hirose T, Kawamori R: **Effects of diet and exercise on muscle and liver intracellular lipid contents and insulin sensitivity in type 2 diabetic patients.** *J Clin Endocrinol Metab* 2005, **90**:3191–3196.
18. Ohkura T, Shiochi H, Fujioka Y, Sumi K, Yamamoto N, Matsuzawa K, Izawa S, Kinoshita H, Ohkura H, Kato M, Taniguchi SI, Yamamoto K: **20/(fasting C-peptide x fasting plasma glucose) is a simple and effective index of insulin resistance in patients with type 2 diabetes mellitus: a preliminary report.** *Cardiovasc Diabetol* 2013, **12**:21.
19. Inohara H, Segawa T, Miyauchi A, Yoshii T, Nakahara S, Raz A, Maeda M, Miyoshi E, Kinoshita N, Yoshida H, Furukawa M, Takenaka Y, Takamura Y, Ito Y, Taniguchi N: **Cytoplasmic and serum galectin-3 in diagnosis of thyroid malignancies.** *Biochem Biophys Res Commun* 2008, **376**:605–610.
20. Matthews DR, Hosker JP, Rudenski AS, Naylor BA, Treacher DF, Turner RC: **Homeostasis model assessment: insulin resistance and beta-cell function from fasting plasma glucose and insulin concentrations in man.** *Diabetologia* 1985, **28**:412–419.
21. Matsuda M, DeFronzo RA: **Insulin sensitivity indices obtained from oral glucose tolerance testing: comparison with the euglycemic insulin clamp.** *Diabetes Care* 1999, **22**:1462–1470.
22. Seltzer HS, Allen EW, Herron AL Jr, Brennan MT: **Insulin secretion in response to glycemic stimulus: relation of delayed initial release to carbohydrate intolerance in mild diabetes mellitus.** *J Clin Invest* 1967, **46**:323–335.
23. Hong EG, Ko HJ, Cho YR, Kim HJ, Ma Z, Yu TY, Friedline RH, Kurt-Jones E, Finberg R, Fischer MA, Granger EL, Norbury CC, Hauschka SD, Philbrick WM, Lee CG, Elias JA, Kim JK: **Interleukin-10 prevents diet induced insulin resistance by attenuating macrophage and cytokine response in skeletal muscle.** *Diabetes* 2009, **58**:2525–2535.
24. Zhu W, Sano H, Nagai R, Fukuhara K, Miyazaki A, Horiuchi S: **The role of galectin-3 in endocytosis of advanced glycation end products and modified low density lipoproteins.** *Biochem Biophys Res Commun* 2001, **280**:1183–1188.
25. Iacobini C, Menini S, Ricci C, Scipioni A, Sansoni V, Cordone S, Taurino M, Serino M, Marano G, Federici M, Pricci F, Pugliese G: **Accelerated lipid-induced atherogenesis in galectin-3-deficient mice: role of lipoxidation via receptor-mediated mechanisms.** *Arterioscler Thromb Vasc Biol* 2009, **29**:831–836.

doi:10.1186/1758-5996-6-106
Cite this article as: Ohkura *et al.*: Low serum galectin-3 concentrations are associated with insulin resistance in patients with type 2 diabetes mellitus. *Diabetology & Metabolic Syndrome* 2014 **6**:106.

Clinical Translational Research

Oncology

Oncology
DOI: 10.1159/000369495

Received: May 26, 2014
Accepted after revision: October 30, 2014
Published online: January 7, 2015

Expression of Fucosyltransferase 8 Is Associated with an Unfavorable Clinical Outcome in Non-Small Cell Lung Cancers

Rio Honma[a] Ichiro Kinoshita[a] Eiji Miyoshi[e] Utano Tomaru[b] Yoshihiro Matsuno[d] Yasushi Shimizu[a] Satoshi Takeuchi[a] Yuka Kobayashi[f] Kichizo Kaga[c] Naoyuki Taniguchi[g] Hirotoshi Dosaka-Akita[a]

Departments of [a]Medical Oncology, [b]Pathology and [c]Cardiovascular and Thoracic Surgery, Hokkaido University Graduate School of Medicine, and [d]Department of Surgical Pathology, Hokkaido University Hospital, Sapporo, [e]Department of Molecular Biochemistry and Clinical Investigation, Osaka University Graduate School of Medicine, Suita, [f]J-Oil Mills, Inc., Yokohama, and [g]Systems Glycobiology Research Group, RIKEN-Max Planck Joint Research Center, Riken Global Research Cluster, Wako, Japan

Key Words
Fucosyltransferase 8 · Non-small cell lung cancers · Prognosis · Histology

Abstract
Objecitive: Fucosyltransferase 8 (FUT8), the only enzyme responsible for the core α1,6-fucosylation of asparagine-linked oligosaccharides of glycoproteins, is a vital enzyme in cancer development and progression. We examined FUT8 expression in non-small cell lung cancers (NSCLCs) to analyze its clinical significance. We also examined the expression of guanosine diphosphate-mannose-4,6-dehydratase (GMD), which is imperative for the synthesis of fucosylated oligosaccharides. ***Methods:*** Using immunohistochemistry, we evaluated the expression of FUT8 and GMD in relation to patient survival and prognosis in potentially curatively resected NSCLCs. ***Results:*** High expression of FUT8 was found in 67 of 129 NSCLCs (51.9%) and was significantly found in non-squamous cell carcinomas ($p = 0.008$). High expression of FUT8 was associated with poor survival ($p = 0.03$) and was also a significant and independent unfavorable prognostic factor in patients with potentially curatively resected NSCLCs ($p = 0.047$). High expression of GMD was significantly associated with high FUT8 expression ($p = 0.04$). ***Conclusions:*** High expression of FUT8 is associated with an unfavorable clinical outcome in patients with potentially curatively resected NSCLCs, suggesting that FUT8 can be a prognostic factor. The analysis of FUT8 expression and its core fucosylated products may provide new insights for the therapeutic targets of NSCLCs.

Introduction

Lung cancer is a leading cause of cancer death throughout the world. Over 80% of patients with lung cancer have non-small cell lung cancer (NSCLC). Although the management and treatment of NSCLCs have improved, there is little evidence to suggest that therapeutic advances have resulted in a marked increase in survival rates, and the overall 5-year survival rate remains around 15% [1, 2]. Patients with NSCLCs at comparable stages may have different clinical courses and respond differently to similar treatments, but the reasons for these differences are not

KARGER 125

0030–2414/15/0000–0000$39.50/0

E-Mail karger@karger.com
www.karger.com/ocl

Prof. Hirotoshi Dosaka-Akita
Department of Medical Oncology
Hokkaido University Graduate School of Medicine
North 15, West 7, Kita-ku, Sapporo 060-8638 (Japan)
E-Mail hdakita@med.hokudai.ac.jp

fully understood. A more sophisticated understanding of the pathogenesis and biology of these tumors may aid in histological diagnosis, predicting clinical outcome, individualizing treatment, and identifying molecular targets of the treatment [3–8].

Recent advances in glycomics have revealed the functional roles of oligosaccharides and their effect on human diseases [9]. Many studies show that alterations in asparagine-linked oligosaccharides of tumor cells are associated with carcinogenesis, invasion, and metastasis [10–12]. Among 13 fucosyltransferases known to be encoded by the human genome, fucosyltransferase 8 (FUT8) is the only enzyme to catalyze the transfer of a fucosyl moiety from guanosine diphosphate (GDP)-fucose to the innermost GlcNAc residue of hybrid and complex asparagine-linked oligosaccharides in glycoprotein via α1,6 linkage to form core fucosylation, which is frequently observed in malignant transformation [13–18]. Increased FUT8 activity is certainly an important factor in the regulation of fucosylation, although other factors may be involved in its regulation, such as the synthesis of GDP-L-fucose (GDP-L-Fuc), the substrate for FUT8. GDP-L-Fuc is synthesized in the cytosol through both a salvage and, mainly, a de novo pathway [19], which involves the conversion of cellular GDP-D-mannose into GDP-L-Fuc by GDP-mannose-4,6-dehydratase (GMD) [20] and GDP-4-keto-6-deoxy-D-mannose-3,5-epimerase-4-reductase (GDP-L-Fuc synthase).

In the present study, we immunohistochemically examined FUT8 expression in NSCLCs. To clarify the association of FUT8 expression with malignant properties of lung cancers, we examined the survival of patients with potentially curatively resected NSCLCs. We also analyzed the expression of GMD, which is imperative for the synthesis of all fucosylated oligosaccharides [20].

Materials and Methods

Tumor Specimens and Survival Data

Tumor tissues were collected from 129 patients with NSCLCs who underwent surgery at Hokkaido University Hospital between 1981 and 1994. Of the 129 cases of NSCLCs, 51 were squamous cell carcinomas (SCCs), 71 were adenocarcinomas, 6 were adenosquamous cell carcinomas, and 1 case was a large cell carcinoma. All cases were diagnosed based on the 1982 WHO classification, and the pathological diagnoses were confirmed according to the 2004 WHO classification. The postsurgical pathological tumor-node-metastasis stage (pTNM) was determined according to the guidelines of the American Joint Committee on Cancer [21]. Of the 129 patients, 107 were potentially curatively resected, and survival analysis was performed in 95 patients who met the following criteria: (a) survived for >3 months after surgery; (b) did not die of causes other than lung cancer within 5 years after surgery, and (c) were followed for >3 years after surgery (for patients who remained alive). Of the 107 patients, 12 did not meet these criteria and were therefore excluded from the survival analysis. This study was approved by the Medical Ethics Committee of Hokkaido University Hospital.

Cell Lines and Western Blot

Immortalized cell lines established from human bronchial epithelial cells, HBEC3-KT and BEAS-2B, were provided by John D. Minna (University of Texas Southwestern Medical Center, Dallas, Tex., USA) and the American Type Culture Collection (Manassas, Va., USA), respectively. Three human NSCLC cell lines, NCI-H520, HCC827, and NCI-H1975, were purchased from the American Type Culture Collection, and one NSCLC cell line, PC-3, was provided by the Japan Cancer Research Resources Bank (Tokyo, Japan). Cells were lysed in a buffer containing 150 mM NaCl, 20 mM Tris-HCl (pH 7.5), 0.2% NP-40, and 1 mM DTT, and they were centrifuged at 15,000 *g* for 10 min. The supernatants (20-μg aliquot of total proteins) were subjected to SDS-PAGE and blotted to nitrocellulose membranes. The blots were probed with a mouse monoclonal antibody (Ab) against recombinant human FUT8 (15C6, 1:2,000 dilution; Fujirebio Inc., Tokyo, Japan) [15], a rabbit polyclonal Ab against recombinant human GMD (1:200 dilution; generated by E.M.) [22], or actin Ab (Abcam, Tokyo, Japan), and reacted with horseradish peroxidase-conjugated anti-mouse or anti-rabbit IgG (Jackson ImmunoResearch, West Grove, Pa., USA) for immunodetection. The immune complexes were visualized by enhanced chemiluminescence (Amersham, Piscataway, N.J., USA) and analyzed by Image Gauge software (Fujifilm, Tokyo, Japan).

Immunohistochemistry for FUT8 and GMD

Formalin-fixed tissue sections or cell clot sections were deparaffinized in xylene and rehydrated in graded alcohols and distilled water. For the immunohistochemical detection of FUT8, tissue slides were processed for antigen retrieval by a standard microwave heating technique. After blocking, the sections were subsequently incubated with FUT8 Ab (1:1,600 dilution) [15], GMD Ab (1:100 dilution) [22], or control mouse isotype-specific immunoglobulin at 4°C overnight. Immunostaining was performed by the biotin-streptavidin immunoperoxidase method (SAB-PO kit; Nichirei, Tokyo, Japan). Formalin-fixed tissue sections were also stained with hematoxylin and eosin (HE).

Criteria for Immunohistochemical Staining of FUT8 and GMD

Immunohistochemical staining for FUT8 and GMD was assessed by the percentage of stained tumor cells per slide (0–100%) and the predominant level of staining intensity (0 = negative, 1 = weak, 2 = intermediate, and 3 = strong). Immunostaining was interpreted as high when more than 30% of the tumor cells exhibited intensity 2 or 3 for evaluating the excessive expression of FUT8 in tumor cells. Cases with negative, weak, and focal staining with intensity 2 or 3 were evaluated as low. All cases of immunohistochemical staining were independently analyzed by R.H., U.T., and H.D.-A.

Pholiota Squarrosa Lectin Histochemistry

The expression of core α1,6-fucosylated asparagine-linked oligosaccharides (glycans) was analyzed by *Pholiota squarrosa* lectin

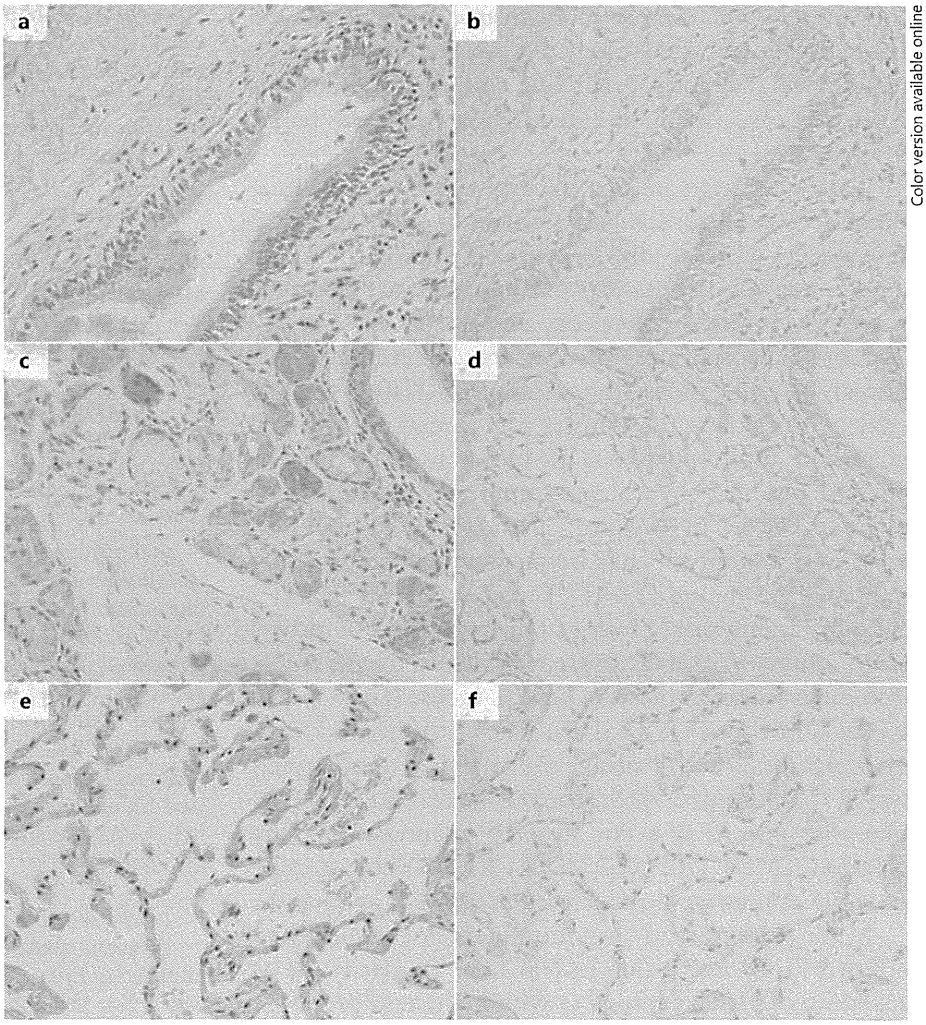

Color version available online

Fig. 1. Expression of FUT8 in normal lung tissues. Representative immunostaining for FUT8 expression in normal lung tissues. Bronchial epithelial cells (**a**, **b**) and bronchial gland cells (**c**, **d**) frequently showed weak expression of FUT8. **e**, **f** FUT8 expression was rarely found in flat alveolar epithelial cells. Sections were stained with HE (**a**, **c**, **e**) and immunostained for FUT8 (**b**, **d**, **f**).

(PhoSL) histochemistry [23]. After deparaffinization, the labeled biotin-streptavidin method was used on 4-μm-thick sections of formalin-fixed paraffin-embedded tissues, which were consecutively made for immunohistochemistry for FUT8 and GMD as well as PhoSL histochemistry. After blocking nonspecific staining, the sections were subsequently incubated with 1 μg/ml biotinylated PhoSL for 1 h at room temperature. Staining was performed by the biotin-streptavidin immunoperoxidase method with 3,3′-diaminobenzidine as a chromogen (SAB-PO kit; Nichirei). Hematoxylin was used as a counterstain. For negative controls, Tween-20 TBS was used instead of PhoSL.

PhoSL binding reactivity was classified based on the percentage of positively stained cancer cells (≥50% = high; ≥10 and <50% = moderate, or <10% = low).

Statistical Analyses

The relationship between FUT8 or GMD expression and age was analyzed by Student's t test. The correlation of FUT8 or GMD expression with other clinicopathological parameters was analyzed by the χ^2 test or Fisher's exact test, as appropriate. Univariate and multivariate analyses were performed using StatView software (SAS Institute Inc., Cary, N.C., USA). Survival curves were estimated by using the Kaplan-Meier method, and differences in survival distributions were evaluated by the log-rank test. Cox's proportional hazards model was used to identify factors that might have a significant influence on survival. p values <0.05 were considered statistically significant. All tests were two-sided.

Results

Expression of FUT8 and GMD in Normal Lung Tissues and NSCLC Cell Lines

In normal lung tissues, bronchial epithelial cells and bronchial gland cells frequently showed weak expression of FUT8 and GMD, which served as internal positive control (fig. 1; online suppl. fig. 1; for all online suppl. material, see www.karger.com/doi/10.1159/000369495). The

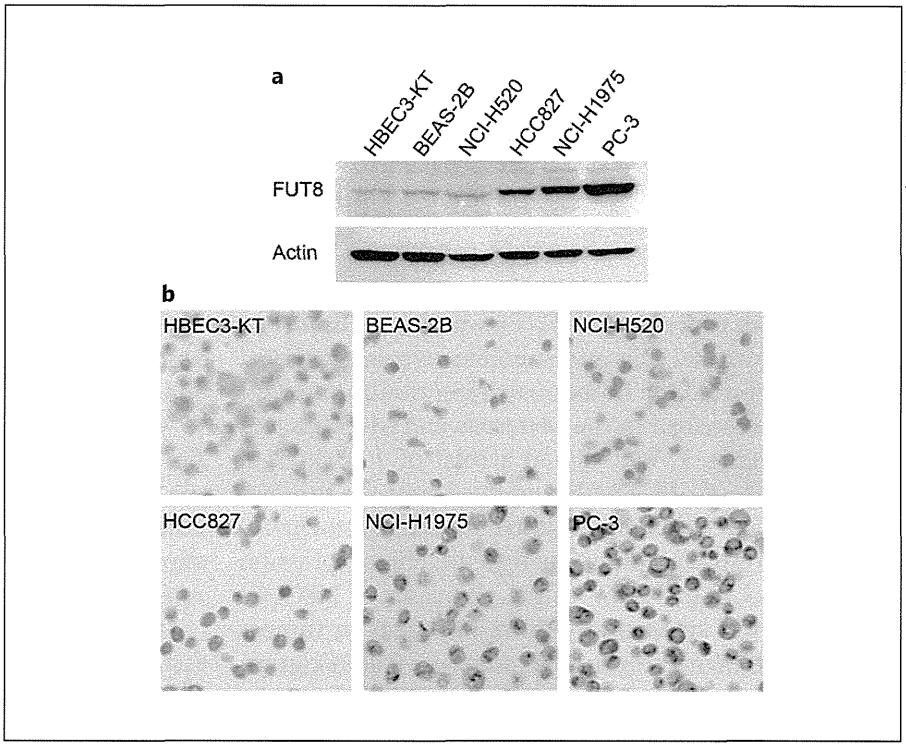

Color version available online

Fig. 2. Levels of immunostaining intensity for FUT8. Expression of FUT8 in NSCLC cell lines as examined by Western blot (**a**) and immunohistochemical staining (**b**). HBEC3-KT and BEAS-2B are immortalized cell lines established from human bronchial epithelial cells. NCI-H520, HCC827, NCI-H1975, and PC-3 are cancer cell lines derived from NSCLCs.

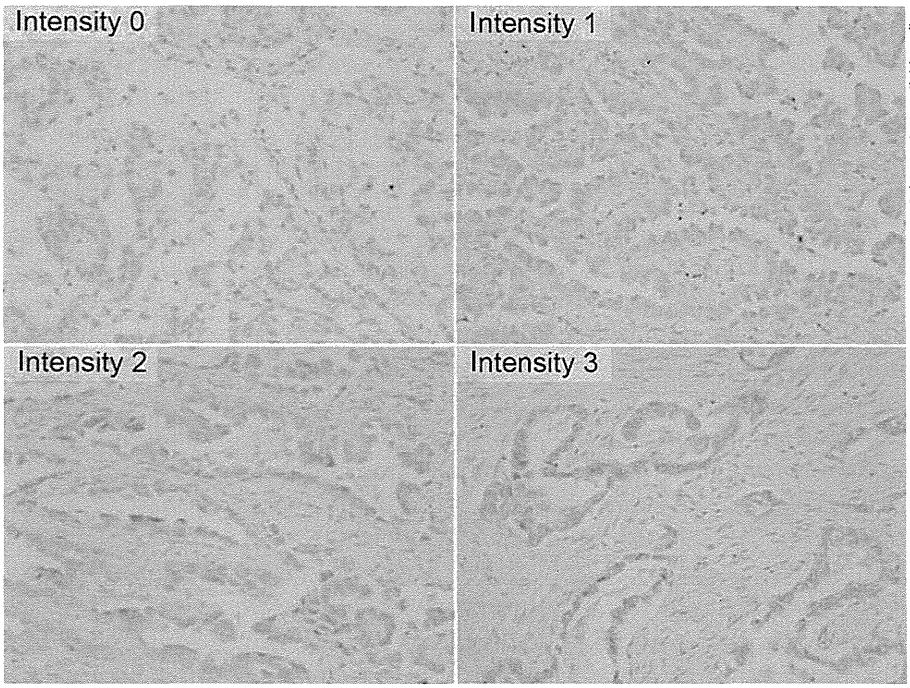

Color version available online

Fig. 3. Levels of immunostaining intensity for FUT8. Immunostaining for FUT8 in tumors. 0 = Negative; 1 = weak; 2 = intermediate, and 3 = strong. Immunostaining for GMD was evaluated in the same manner.

expression of FUT8 and GMD was rarely found in flat alveolar epithelial cells (fig. 1; online suppl. fig. 1). Weak expression of FUT8 was partly observed in reactive cuboidal alveolar epithelial cells around inflammatory foci (online suppl. fig. 2). To confirm a correlation between the level of protein expression and immunostaining, we performed in vitro experiments using human cell lines derived from immortalized bronchial epithelial cells and NSCLCs. As shown in figure 2, increased expression of FUT8 was observed in some NSCLC cell lines by Western

blot, and these cell lines showed strong immunostaining for FUT8, in comparison with cell lines with weak expression of FUT8. For GMD expression, we found similar results (data not shown). These results indicated that immunohistochemical analyses using FUT8 and GMD Abs could be utilized to evaluate the expression levels of these molecules.

Expression of FUT8 in NSCLCs

Since weak expression of FUT8 was found in normal bronchial epithelial cells and cuboidal alveolar epithelial cells, we evaluated the immunostaining results based on the criteria described in the Materials and Methods and shown in figure 3. We stained a total of 129 cases of NSCLCs with anti-FUT8 Ab, and the results are summarized in table 1. The representative immunohistochemical staining results are shown in figure 4. High expression of FUT8 was found in 67 of the 129 cases of NSCLCs (51.9%). It was significantly more prevalent in tumors from women than in those from men ($p < 0.0001$), in tumors from nonsmokers than in those from smokers ($p = 0.002$), in non-SCCs than in SCCs ($p < 0.0001$), and in well-differentiated tumors than in poorly differentiated tumors ($p = 0.02$; table 1a). In multivariate logistic regression analysis for the correlation of FUT8 expression with various parameters, FUT8 expression was relevant to histological type: it was significantly found in non-SCC, compared with SCC cases (odds ratio 3.51, $p = 0.008$; table 1b).

Since adenocarcinoma was a major histological type among the non-SCC cases, we then separately analyzed the correlation of FUT8 expression with clinical and clinicopathological parameters in the cases with adenocarcinoma (table 1). In patients with adenocarcinoma, high expression of FUT8 was significantly more prevalent in tumors from women than in those from men ($p = 0.03$), in tumors from nonsmokers than in those from smokers ($p = 0.049$), and in tumors with pN1–3 than in those with pN0 ($p = 0.01$; table 1a). In multivariate logistic regression analysis, high expression of FUT8 was related to lymph node metastasis; FUT8 expression was found to be significant in cases with pN1–3 as compared to those with pN0 (odds ratio 5.95, $p = 0.02$; table 1b). FUT8 expression did not show any correlation with various parameters in the SCC cases.

Expression of FUT8 Correlates with Patient Survival and Prognosis in NSCLCs

We next analyzed the relationship between FUT8 expression and patient survival (fig. 5). In 95 cases of potentially curatively resected NSCLCs, the survival of patients with high expression of FUT8 was significantly shorter than that of patients with low expression of FUT8 (5-year survival rates, 48 and 66%, respectively; $p = 0.03$; fig. 5a). In addition, even in 65 cases of NSCLCs with pStage I, the survival of patients with high expression of FUT8 was significantly shorter than that of patients with low expression of FUT8 (5-year survival rates, 60 and 83%, respectively; $p = 0.03$; fig. 5b). In 55 cases of potentially curatively resected adenocarcinoma, the survival of patients with high expression of FUT8 was also significantly shorter than that of patients with low expression of FUT8 (5-year survival rates, 49 and 79%, respectively; $p = 0.009$; fig. 5c). Strikingly, in 37 cases of pStage I adenocarcinoma, none of the 15 patients with low expression of FUT8 died of lung cancer, while 11 of the 22 patients with high expression of FUT8 died of lung cancer (5-year survival rates, 100 and 68%, respectively; fig. 5d).

The importance of FUT8 expression as a prognostic factor was analyzed in patients with potentially curatively resected NSCLCs (table 2). In univariate analysis, high expression of FUT8 ($p = 0.03$) and advanced pN classification ($p < 0.0001$) were significant as unfavorable prognostic factors (table 2a). In multivariate analysis, high expression of FUT8 and advanced pN classification remained significant (hazard ratio 1.81, $p = 0.047$, and hazard ratio 2.81, $p = 0.0008$, respectively; table 2a). Moreover, univariate analysis of patients with pStage I NSCLCs indicated that high expression of FUT8 was the only significant parameter for unfavorable prognosis (hazard ratio 2.55, $p = 0.03$; table 2b).

Expression of GMD in NSCLCs

High expression of GMD was found in 96 of the 129 cases of NSCLC (74.4%; table 3). The representative immunohistochemical staining results are shown in figure 4. GMD expression was significantly more prevalent in non-SCC than in SCC cases ($p = 0.004$; table 3). In multivariate logistic regression analysis for the correlation of GMD expression with various parameters, high expression of GMD was found to be significant in non-SCC as compared with SCC cases (odds ratio 2.80, $p = 0.03$). High expression of GMD was significantly more prevalent in cases with high expression of FUT8 than in those with low expression of FUT8 ($p = 0.04$; table 3), indicating that the coexpression of FUT8 and GMD frequently occurred in the tumor cells of NSCLCs. GMD expression did not correlate with survival or prognosis (table 2; data not shown).

Table 1. FUT8 expression in overall NSCLCs and adenocarcinomas

a Analysis by the χ^2 test, Fisher's exact test, or Student's t test

Characteristics	FUT8 expression (NSCLCs)			FUT8 expression (adenocarcinomas)		
	low (n = 62)	high (n = 67)	p	low (n = 21)	high (n = 50)	p
Mean age ± SD, years	64.1±8.1	63.7±11.1	0.8	62.4±7.6	62.7±11.7	0.9
Sex						
Male	52	33	<0.0001	14	19	0.03
Female	10	34		7	31	
Smoking						
Nonsmoker	9	25	0.002	6	23	0.049
Smoker	49	33		15	19	
Histology						
SCC	38	13	<0.0001			
Adenocarcinoma	21	50				
Others[a]	3	4				
Differentiation						
Well	12	23	0.02	8	22	0.2
Moderate	25	30		6	20	
Poor	22	10		6	6	
pT classification						
1	13	22	0.2	5	18	0.3
2–4	48	45		16	32	
pN classification						
0	45	40	0.1	18	27	0.01
1–3	16	27		3	23	
pM classification						
0	60	65	0.6	21	49	0.5
1	1	2		0	1	
pStage						
I	39	38	0.7[b]	15	27	0.2[b]
II	5	6		0	6	
IIIa	17	20		6	15	
IIIb	0	1		0	1	
IV	1	2		0	1	

Values are numbers unless indicated otherwise. [a] Large cell carcinoma and adenosquamous cell carcinoma. [b] pStage I versus II–IV.

b Multivariate logistic regression analysis

Characteristics	NSCLCs		Adenocarcinomas	
	odds ratio	p	odds ratio	p
Sex (female vs. male)	2.36	0.2	2.61	0.3
Smoking (nonsmoker vs. smoker)	1.07	0.9	1.74	0.5
Histology (non-SCC vs. SCC)	3.51	0.008		
Differentiation (well/moderate vs. poor)	1.43	0.5		
pN classification (N1–3 vs. N0)			5.95	0.02

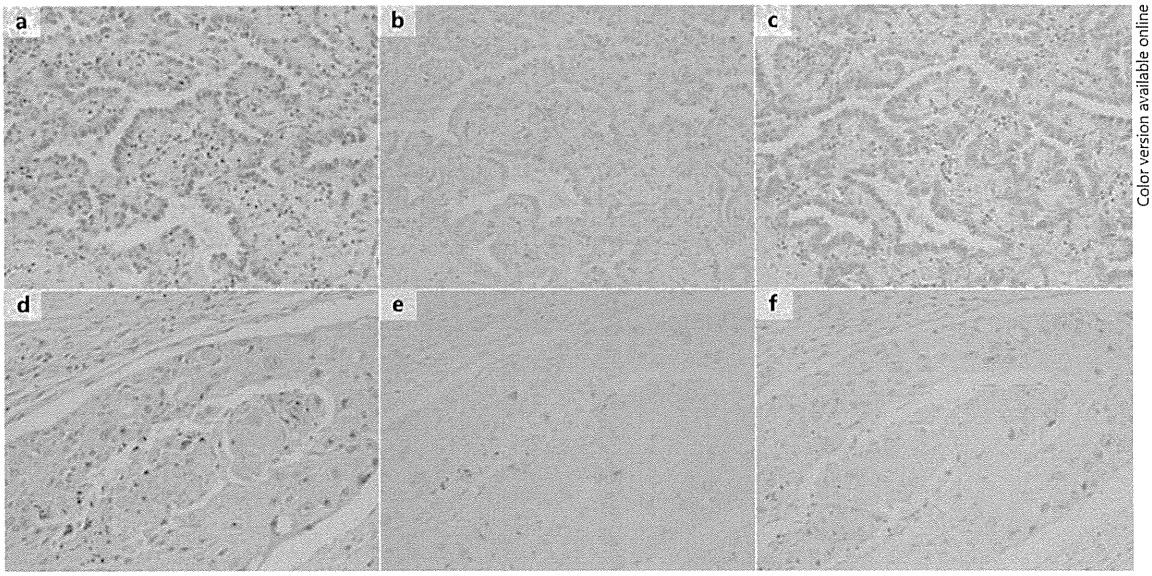

Fig. 4. Expression of FUT8 and GMD in NSCLCs. Representative immunostaining of FUT8 and GMD in 2 tumors: an adenocarcinoma (**a–c**) and a SCC (**d–f**). HE staining (**a**, **d**) and immunostaining for FUT8 (**b**, **e**) and GMD (**c**, **f**).

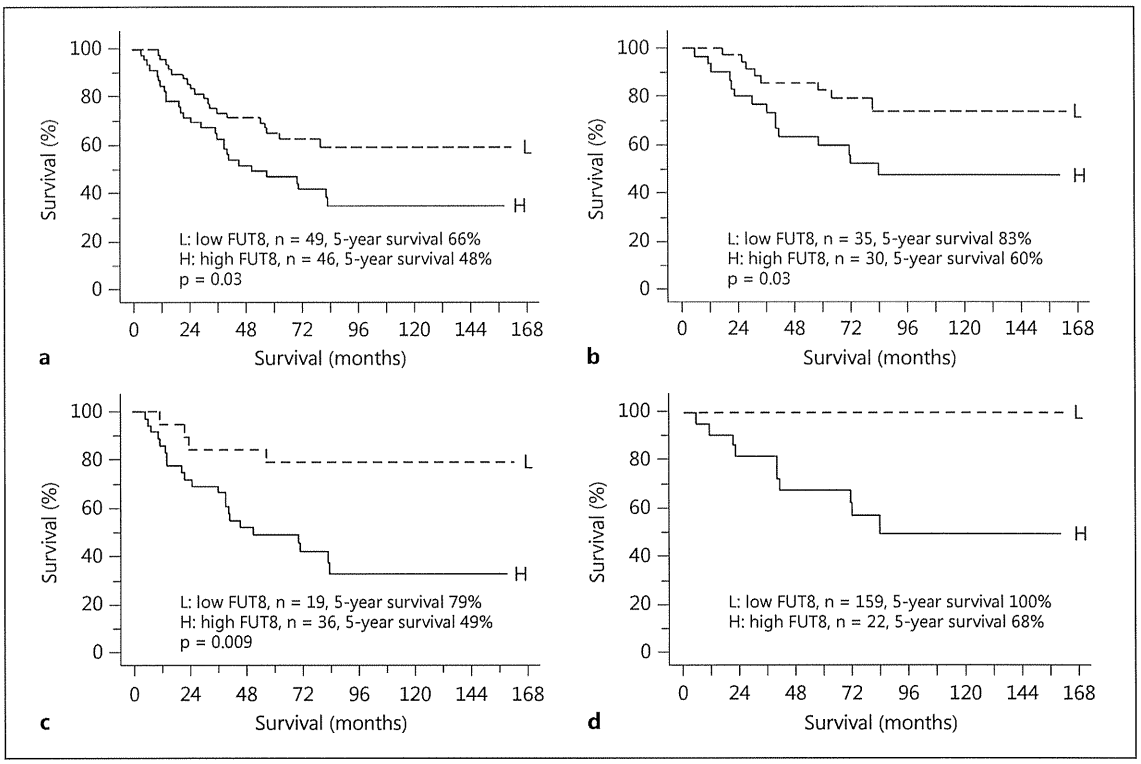

Fig. 5. Kaplan-Meier survival curves for patients with NSCLCs. The survival curves for patients with curatively resected tumors (**a**, **c**) and for patients with pStage I tumors (**b**, **d**) are stratified by high and low expression of FUT8 in NSCLCs overall (**a**, **b**) and in adenocarcinomas (**c**, **d**). **d** The differences in survival distributions between patients with high and low expression of FUT8 could not be statistically analyzed since no patients with pStage I adenocarcinomas having low FUT8 expression died (no events occurred).

Table 2. Cox proportional hazards model analysis of prognostic factors

a Patients with curatively resected NSCLCs

Characteristics	Hazard ratio	95% CI	p
Univariate analysis of potential prognostic factors			
Sex (female vs. male)	0.66	0.43–1.03	0.07
Age (≥65 vs. <65 years)	1.19	0.79–1.77	0.4
Histology (non-SCC vs. SCC)	0.98	0.65–1.47	0.9
Differentiation (poor vs. well/moderate)	0.93	0.55–1.59	0.8
pT classification (T2–4 vs. T1)	1.04	0.69–1.58	0.9
pN classification (N1–3 vs. N0)	2.26	1.51–3.40	<0.0001
FUT8 expression (high vs. low)	1.93	1.07–3.45	0.03
GMD expression (high vs. low)	1.71	0.80–3.65	0.2
Multivariate analysis of prognostic factors			
pN classification (N1–3 vs. N0)	2.81	1.54–5.13	0.0008
FUT8 (high vs. low)	1.81	1.01–3.25	0.047

b Patients with pStage I NSCLCs

Characteristics	Hazard ratio	95% CI	p
Univariate analysis of potential prognostic factors			
Sex (female vs. male)	0.60	0.32–1.12	0.1
Age (≥65 vs. <65 years)	1.28	0.73–2.24	0.4
Histology (non-SCC vs. SCC)	0.73	0.42–1.28	0.3
Differentiation (poor vs. well/moderate)	0.85	0.37–1.96	0.7
pT classification (T2–4 vs. T1)	0.80	0.46–1.40	0.4
FUT8 expression (high vs. low)	2.55	1.08–6.03	0.03
GMD expression (high vs. low)	1.78	0.61–5.23	0.3

PhoSL Histochemical Staining in NSCLCs

The expression of core α1,6-fucosylated asparagine-linked oligosaccharides was analyzed by PhoSL histochemistry. PhoSL is a reliable reagent to detect specifically core α1,6-fucosylated asparagine-linked oligosaccharides [23]. NSCLCs with both high and low expression of FUT8 and GMD were used for PhoSL histochemistry to determine whether FUT8 and GMD expression resulted in the synthesis of core α1,6-fucosylated asparagine-linked oligosaccharides (online suppl. fig. 3). PhoSL-positive staining was observed significantly more frequently in tumors with high expression of both FUT8 and GMD, compared with tumors with low expression of both FUT8 and GMD ($p = 0.02$). Among the 8 NSCLCs with high expression of both FUT8 and GMD, 6 showed high PhoSL staining and 2 showed moderate PhoSL staining. However, among the 9 NSCLCs with low expression of both FUT8 and GMD, 6 showed low PhoSL staining, and 1 showed moderate PhoSL staining.

Discussion

In the present study, we demonstrated that high expression of FUT8 is observed in about half of the NSCLC cases. It is more frequently found in non-SCC than in SCC cases. Furthermore, high expression of FUT8 is associated with a shorter survival period and is an unfavorable prognostic factor in cases with potentially curatively resected and pStage I NSCLCs.

Oligosaccharides are synthesized by a set of several glycosyltransferases. Among them, FUT8 and *N*-acetylglucosaminyltransferase V (GnT-V) have been shown to be involved in cancer development and progression [13, 14, 24]. Previously, we have demonstrated that GnT-V expression is associated with the histological type and prognosis in patients with NSCLCs [25]. Low expression of GnT-V was more frequently found in SCC than in non-SCC cases. The survival of patients with low expression of GnT-V was shorter than that of patients with high ex-

Table 3. GMD expression in overall NSCLCs and adenocarcinomas

Characteristics	GMD expression (NSCLCs)			GMD expression (adenocarcinomas)		
	low (n = 33)	high (n = 96)	p	low (n = 11)	high (n = 60)	p
Mean age ± SD, years	64.6±9.5	63.6±9.9	0.6	63.5±12.1	62.4±10.4	0.8
Sex						
Male	26	59	0.07	6	27	0.6
Female	7	37		5	33	
Smoking						
Nonsmoker	5	29	0.1	3	26	0.4
Smoker	24	58		6	28	
Histology						
SCC	20	31	0.004			
Adenocarcinoma	11	60				
Others[a]	2			0		
Differentiation						
Well	8	27	0.3	5	25	0.4
Moderate	14	41		3	23	
Poor	11	21		3	9	
pT classification						
1	12	23	0.2	5	18	0.3
2–4	21	72		6	42	
pN classification						
0	22	63	0.97	7	38	0.98
1–3	11	32		4	22	
pM classification						
0	33	92	0.6	11	59	0.7
1	0	3		0	1	
pStage						
I	20	57	0.9[b]	7	35	0.8[b]
II	3	8		1	5	
IIIa	10	27		3	18	
IIIb	0	1		0	1	
IV	0	3		0	1	
FUT8 expression						
Low	21	41	0.04			
High	12	55				

Values are numbers unless indicated otherwise. [a] Large cell carcinoma and adenosquamous cell carcinoma. [b] pStage I vs. II–IV.

pression of GnT-V. However, FUT8 expression has not been widely examined in lung cancer.

FUT8 is the only enzyme responsible for the core α1,6-fucosylation, which is involved in the regulation of protein functions [14]. Although detailed molecular mechanisms of FUT8 involved in tumor progression remain to be determined, core α1,6-fucosylation is crucial for the ligand binding affinity of epidermal growth factor receptor and transforming growth factor β_1 receptor, and it enhances the downstream signals to induce tumor growth, invasion, and metastasis [26, 27]. Loss of core fucose on epidermal growth factor receptor and transforming growth factor β_1 receptor reduces the ligand binding ability as well as downstream signaling [26, 27]. Recently, Chen et al. [28]

have reported that expression of FUT8 is involved in the malignant behaviors of lung cancer cell lines, including in vitro invasion and cell proliferation, as well as in vivo metastasis and tumor growth. Using glycoproteomic and microarray analyses, they have shown that FUT8 globally modifies cell surface antigens, receptors, and adhesion molecules and that it is involved in the regulation of many genes associated with malignancy, suggesting that FUT8 contributes to tumor progression through multiple mechanisms. Consistent with our present observation, they also reported that expression of FUT8 correlated with poor survival in patients with NSCLCs. However, their analyses included cases with noncurative and curative resection, and 45 of 140 cases (32%) were classified as stage IV with metastasis [28]. In the present study, we have clarified for the first time that expression of FUT8 correlates with a short survival period and poor prognosis in patients with curatively resected and pStage I NSCLCs.

In addition to FUT8, GMD is a key enzyme for core α1,6-fucosylation [20]. GMD expression was also found in NSCLCs, although it was not associated with survival or prognosis (table 2; data not shown). Similar to FUT8 expression, high expression of GMD was significantly found in non-SCC cases. High expression of GMD was more prevalent in cases with high expression of FUT8, indicating that concordant expression of FUT8 and GMD frequently occurred in NSCLCs (table 3). When we stained tumor sections using PhoSL to detect specifically core α1,6-fucosylated asparagine-linked oligosaccharides [23], PhoSL-positive cells were observed more frequently in tumors with high expression of both FUT8 and GMD than in those with low expression of both FUT8 and GMD (online suppl. fig. 3). Therefore, it is expected that expression of both FUT8 and GMD results in the synthesis of core α1,6-fucosylated asparagine-linked oligosaccharides in the tumor cells of NSCLCs.

The upregulation of FUT8 has been observed in several types of malignancy, including liver, ovarian, thyroid, and colorectal cancers [15–18]. In thyroid papillary carcinomas, high expression of FUT8 is linked to tumor size and lymph node metastasis [15]. In colorectal cancers, the expression of FUT8 is considerably higher in cancer cells than in normal epithelial cells. It correlates with the advanced pStage and poor prognosis [18, 29]. Fucosylated haptoglobin is a novel type of cancer biomarker with a prognostic value after an operation for colorectal cancer [30]. Taken together, these observations suggest that the alteration of core fucosylation following FUT8 expression relates to the progression of cancers. Further study should address the molecular mechanisms involved in aberrant expression of FUT8 in tumor cells to find therapeutic targets for NSCLCs and other cancers.

In conclusion, we have demonstrated for the first time that high expression of FUT8 correlates with an unfavorable clinical outcome in patients with potentially curatively resected and pStage I NSCLCs, suggesting that FUT8 can be a prognostic factor. Further analysis of FUT8 expression and its core-fucosylated products may provide new insights into the therapeutic targets of NSCLCs.

Acknowledgements

This work was supported in part by a Grant-in-Aid (No. 22501029) from the Ministry of Education, Science, Sports and Culture of Japan.

Disclosure Statement

The authors declare no conflicts of interest.

References

1 NSCLC Meta-Analyses Collaborative Group: Chemotherapy in addition to supportive care improves survival in advanced non-small-cell lung cancer: a systematic review and meta-analysis of individual patient data from 16 randomized controlled trials. J Clin Oncol 2008;26:4617–4625.

2 Grossi F, Aita M, Defferrari C, Rosetti F, Brianti A, Fasola G, Vinante O, Pronzato P, Pappagallo G: Impact of third-generation drugs on the activity of first-line chemotherapy in advanced non-small cell lung cancer: a meta-analytical approach. Oncologist 2009;14:497–510.

3 Kaufman J, Horn L, Carbone D: Molecular biology of lung cancer; in DeVita VT Jr, Lawrence TS, Rosenberg SA (eds): Cancer: Principles and Practice of Oncology, ed 9. Philadelphia, Lippincott Williams & Wilkins, 2011, pp 789–798.

4 Hanahan D, Weinberg RA: Hallmarks of cancer: the next generation. Cell 2011;144:646–674.

5 Dosaka-Akita H, Hommura F, Mishina T, Ogura S, Shimizu M, Katoh H, Kawakami Y: A risk-stratification model of non-small cell lung cancers using cyclin E, Ki-67, and ras p21: different roles of G1 cyclins in cell proliferation and prognosis. Cancer Res 2001;61:2500–2504.

6 Pao W, Girard N: New driver mutations in non-small-cell lung cancer. Lancet Oncol 2011;12:175–180.
7 Gold KA, Wistuba II, Kim ES: New strategies in squamous cell carcinoma of the lung: identification of tumor drivers to personalize therapy. Clin Cancer Res 2012;18:3002–3007.
8 Gibbs JB: Mechanism-based target identification and drug discovery in cancer research. Science 2000;287:1969–1973.
9 Hart GW, Copeland RJ: Glycomics hits the big time. Cell 2010;143:672–676.
10 Hakomori S: Aberrant glycosylation in tumors and tumor-associated carbohydrate antigens. Adv Cancer Res 1989;52:257–331.
11 Varki A: Biological roles of oligosaccharides: all of the theories are correct. Glycobiology 1993;3:97–130.
12 Dwek RA: Glycobiology: Toward understanding the function of sugars. Chem Rev 1996;96:683–720.
13 Lau KS, Dennis JW: N-Glycans in cancer progression. Glycobiology 2008;18:750–760.
14 Miyoshi E, Noda K, Yamaguchi Y, Inoue S, Ikeda Y, Wang W, Ko JH, Uozumi N, Li W, Taniguchi N: The alpha1–6-fucosyltransferase gene and its biological significance. Biochim Biophys Acta 1999;1473:9–20.
15 Ito Y, Miyauchi A, Yoshida H, Uruno T, Nakano K, Takamura Y, Miya A, Kobayashi K, Yokozawa T, Matsuzuka F, Taniguchi N, Matsuura N, Kuma K, Miyoshi E: Expression of alpha1,6-fucosyltransferase (FUT8) in papillary carcinoma of the thyroid: its linkage to biological aggressiveness and anaplastic transformation. Cancer Lett 2003;200:167–172.
16 Hutchinson WL, White YS, Fagan EA, Johnson PJ, Williams R: Impaired binding properties of thyroxine-binding globulin in hepatocellular carcinoma and chronic liver disease. Hepatology 1991;14:116–120.
17 Takahashi T, Ikeda Y, Miyoshi E, Yaginuma Y, Ishikawa M, Taniguchi N: Alpha 1,6 fucosyltransferase is highly and specifically expressed in human ovarian serous adenocarcinomas. Int J Cancer 2000;88:914–919.
18 Muinelo-Romay L, Vazquez-Martin C, Villar-Portela S, Cuevas E, Gil-Martin E, Fernandez-Briera A: Expression and enzyme activity of alpha(1,6)fucosyltransferase in human colorectal cancer. Int J Cancer 2008;123:641–646.
19 Becker DJ, Lowe JB: Fucose: Biosynthesis and biological function in mammals. Glycobiology 2003;13:41R–53R.
20 Ohyama C, Smith PL, Angata K, Fukuda MN, Lowe JB, Fukuda M: Molecular cloning and expression of GDP-D-mannose-4,6-dehydratase, a key enzyme for fucose metabolism defective in Lec13 cells. J Biol Chem 1998;273:14582–14587.
21 Beahrs O, Henson D, Hutter R, Kennedy B (eds): Lung; in: Manual for Staging of Cancer, ed 4. Chicago, American Joint Committee on Cancer, 1992, pp 115–122.
22 Moriwaki K, Noda K, Nakagawa T, Asahi M, Yoshihara H, Taniguchi N, Hayashi N, Miyoshi E: A high expression of GDP-fucose transporter in hepatocellular carcinoma is a key factor for increases in fucosylation. Glycobiology 2007;17:1311–1320.
23 Kobayashi Y, Tateno H, Dohra H, Moriwaki K, Miyoshi E, Hirabayashi J, Kawagishi H: A novel core fucose-specific lectin from the mushroom *Pholiota squarrosa*. J Biol Chem 2012;287:33973–33982.
24 Nakahara S, Saito T, Kondo N, Moriwaki K, Noda K, Ihara S, Takahashi M, Ide Y, Gu J, Inohara H, Katayama T, Tohyama M, Kubo T, Taniguchi N, Miyoshi E: A secreted type of beta1,6 N-acetylglucosaminyltransferase V (GnT-V), a novel angiogenesis inducer, is regulated by gamma-secretase. FASEB J 2006;20:2451–2459.
25 Dosaka-Akita H, Miyoshi E, Suzuki O, Itoh T, Katoh H, Taniguchi N: Expression of N-acetylglucosaminyltransferase V is associated with prognosis and histology in non-small cell lung cancers. Clin Cancer Res 2004;10:1773–1779.
26 Wang X, Gu J, Ihara H, Miyoshi E, Honke K, Taniguchi N: Core fucosylation regulates epidermal growth factor receptor-mediated intracellular signaling. J Biol Chem 2006;281:2572–2577.
27 Wang X, Inoue S, Gu J, Miyoshi E, Noda K, Li W, Mizuno-Horikawa Y, Nakano M, Asahi M, Takahashi M, Uozumi N, Ihara S, Lee SH, Ikeda Y, Yamaguchi Y, Aze Y, Tomiyama Y, Fujii J, Suzuki K, Kondo A, Shapiro SD, Lopez-Otin C, Kuwaki T, Okabe M, Honke K, Taniguchi N: Dysregulation of TGF-beta1 receptor activation leads to abnormal lung development and emphysema-like phenotype in core fucose-deficient mice. Proc Natl Acad Sci USA 2005;102:15791–15796.
28 Chen CY, Jan YH, Juan YH, Yang CJ, Huang MS, Yu CJ, Yang PC, Hsiao M, Hsu TL, Wong CH: Fucosyltransferase 8 as a functional regulator of nonsmall cell lung cancer. Proc Natl Acad Sci USA 2013;110:630–635.
29 Muinelo-Romay L, Villar-Portela S, Cuevas Alvarez E, Gil-Martin E, Fernandez-Briera A: Alpha(1,6)fucosyltransferase expression is an independent prognostic factor for disease-free survival in colorectal carcinoma. Hum Pathol 2011;42:1740–1750.
30 Takeda Y, Shinzaki S, Okudo K, Moriwaki K, Murata K, Miyoshi E: Fucosylated haptoglobin is a novel type of cancer biomarker linked to the prognosis after an operation in colorectal cancer. Cancer 2012;118:3036–3043.

© 2015. Published by The Company of Biologists Ltd | Biology Open (2015) 000, 1–9 doi:10.1242/bio.20148532

RESEARCH ARTICLE

Rab11a is required for apical protein localisation in the intestine

Tomoaki Sobajima[1,2], Shin-ichiro Yoshimura[1], Tomohiko Iwano[1], Masataka Kunii[1,3], Masahiko Watanabe[4], Nur Atik[1], Sotaro Mushiake[5], Eiichi Morii[6], Yoshihisa Koyama[1], Eiji Miyoshi[2] and Akihiro Harada[1,3,*]

ABSTRACT

The small GTPase Rab11 plays an important role in the recycling of proteins to the plasma membrane as well as in polarised transport in epithelial cells and neurons. We generated conditional knockout mice deficient in *Rab11a*. *Rab11a*-deficient mice are embryonic lethal, and brain-specific *Rab11a* knockout mice show no overt abnormalities in brain architecture. In contrast, intestine-specific *Rab11a* knockout mice begin dying approximately 1 week after birth. Apical proteins in the intestines of knockout mice accumulate in the cytoplasm and mislocalise to the basolateral plasma membrane, whereas the localisation of basolateral proteins is unaffected. Shorter microvilli and microvillus inclusion bodies are also observed in the knockout mice. Elevation of a serum starvation marker was also observed, likely caused by the mislocalisation of apical proteins and reduced nutrient uptake. In addition, Rab8a is mislocalised in *Rab11a* knockout mice. Conversely, Rab11a is mislocalised in *Rab8a* knockout mice and in a microvillus atrophy patient, which has a mutation in the *myosin Vb* gene. Our data show an essential role for Rab11a in the localisation of apical proteins in the intestine and demonstrate functional relationships between Rab11a, Rab8a and myosin Vb *in vivo*.

KEY WORDS: Rab11a, Knockout mouse, Cell polarity, Brain, Intestine, Apical membrane

INTRODUCTION

Rab proteins are a subfamily of the Ras superfamily of small GTPases that are known to regulate specific intracellular membrane trafficking pathways. A large number of Rabs are present in a variety of organelles, suggesting that they play roles in defining the nature of these structures. The Rab family is divided into several subfamilies, one of which is the evolutionarily conserved Rab11 subfamily, which is composed of Rab11a, Rab11b, and Rab25 in mammals (Goldenring et al., 1993; Lai et al., 1994) and Ypt31p and Ypt32p in budding yeast *S. cerevisiae* (Benli et al., 1996).

[1]Department of Cell Biology, Graduate School of Medicine, Osaka University, Suita, Osaka, 565-0871, Japan. [2]Department of Molecular Biochemistry and Clinical Investigation, Graduate School of Medicine, Osaka University, Suita, Osaka, 565-0871, Japan. [3]Institute for Molecular and Cellular Regulation, Gunma University, Maebashi, Gunma 371-8512, Japan. [4]Department of Anatomy, Graduate School of Medicine, Hokkaido University, Sapporo, Hokkaido, 060-8638, Japan. [5]Department of Pediatrics, Nara Hospital, Kinki University School of Medicine, Ikoma, Nara, 630-0293, Japan. [6]Department of Pathology, Graduate School of Medicine, Osaka University, Suita, Osaka, 565-0871, Japan.

*Author for correspondence (aharada@acb.med.osaka-u.ac.jp)

Received 15 April 2014; Accepted 29 October 2014

A number of investigations carried out in both polarised and non-polarised cells have demonstrated that Rab11 subfamily proteins are associated with plasma membrane recycling systems, which regulate epithelial polarity and membrane trafficking into and out of the recycling endosome. In non-polarised cells, Rab11a is known to be crucial for recycling, as it has been shown to colocalise with internalised transferrin, and a GDP-bound form of Rab11a perturbs the recycling of transferrin (Ullrich et al., 1996; Ren et al., 1998). In polarised cells, such as epithelial cells, Rab11 family proteins are known to localise to the apical recycling endosome, where they play a role in apical recycling (Goldenring et al., 1996; Casanova et al., 1999; Perez Bay et al., 2013). Furthermore, Rab11 family proteins localise to subapical areas in epithelial cells of the stomach, intestine, and bladder (Goldenring et al., 1994; Goldenring et al., 1996; Khandelwal et al., 2008; Khandelwal et al., 2013). Using primary cultures and tissue cultures, Rab11 proteins were shown to be involved in the exocytosis of discoidal vesicles in bladder umbrella cells (Khandelwal et al., 2008; Khandelwal et al., 2013) and the exocytosis of H^+K^+-ATPase-containing vesicles in stomach parietal cells (Duman et al., 1999). Also, in *C. elegans* oocytes, Rab11 is required for the formation of caveolin-enriched secretory vesicles (Sato et al., 2008). Finally, in *Drosophila*, Rab11 is required for the secretion of rhodopsin in photoreceptor cells (Li et al., 2007).

Rab11 is known to be important for polarisation and vesicular transport in neurons, another type of polarised cell (Shirane and Nakayama, 2006; Takano et al., 2012). However because the Rab11 family includes Rab11a, Rab11b, and Rab25, it is difficult to determine which proteins are necessary for these functions in epithelial cells and neurons. To date, only *Rab25* knockout mice have been generated, which showed increased numbers of intestinal neoplasias when crossed with $APC^{min/+}$ mice (Nam et al., 2010). In this study, we generate brain- and intestine-specific *Rab11a* knockout mice and examine their tissues. Mice lacking Rab11a throughout their entire bodies are embryonic lethal. Brain-specific *Rab11a* knockout mice display no overt phenotypes. However, intestine-specific knockout mice show mislocalisation of apical proteins, microvillus atrophy, and microvillus inclusion bodies. Furthermore, we show that the localisation of Rab8a is altered in *Rab11a* knockout mice. Conversely, the localisation of Rab11a is altered in the intestinal epithelial cells of *Rab8a* knockout mice and in a microvillus atrophy patient, which has a mutation in the *myosin Vb* gene. These results show that Rab11a, Rab8a, and myosin Vb affect the localisation of one another, suggesting close functional relationships between these proteins.

RESULTS

Rab11a knockout mice are embryonic lethal, although brain-specific knockout mice display no overt phenotypes

We generated knockout mice from ES cells ($Rab11a^{tm1a(KOMP)Wtsi}$) provided by the UC Davis KOMP Repository (Fig. 1A,B). When

Biology Open (2015) 000, 1–9 doi:10.1242/bio.20148532

we intercrossed heterozygous knockout mice (*Rab11a*$^{neo/+}$) (Fig. 1C), we were unable to obtain homozygous knockout mice that completely lacked Rab11a throughout the entire body (supplementary material Table S1).

Considering that Rab11a is known to be involved in axonal elongation (Shirane et al., 2006; Takano et al., 2012), we generated brain-specific *Rab11a* knockout (BKO) mice by crossing the *Rab11a*$^{flox/flox}$ mice to *Nestin-Cre* mice (Tronche et al., 1999). The loss of Rab11a specifically in the brains of the BKO mice (*Nestin-Cre; Rab11a*$^{flox/flox}$) was confirmed by Western blot analysis (supplementary material Fig. S1A). Contrary to our expectations, the BKO mice were born at the proper Mendelian frequency (Fig. 1C; supplementary material Table S1) and developed without overt abnormalities. Furthermore, the brains of the BKO mice appeared similar to those of control mice (supplementary material Fig. S1B). To examine the brain development, we performed Nissl staining and immunofluorescence analysis for cortical layer markers, Cux1, which is expressed in the upper layers II–IV and Tbr1, which is expressed in the layers II–IV and VI. In the BKO mice, the neocortex and hippocampus and the positioning of their Cux1- and Tbr1-positive cortical neuron did not show apparent difference from that of the control brains (supplementary material Fig. S1C,D). We further observed no obvious differences in axonal elongation (calbindin), dendritic arborisation (MAP1A or calbindin), distribution of synaptic protein (synaptophysin), and ciliogenesis (Arl13b) in the cerebrum or cerebellum (supplementary material Figs S2, S3). The results of the BKO mice indicated that Rab11a does not have critical role in the neurogenesis and the neuronal maturation.

Intestine-specific *Rab11a* knockout mice display the intracellular accumulation of apical proteins, shortening of microvilli, and microvillus inclusion bodies

To determine the role of Rab11a in the intestinal epithelial cells, we crossed the *Rab11a*$^{flox/flox}$ mice with *Villin-Cre* mice (Madison et al., 2002) (Fig. 1C). We confirmed the loss of Rab11a specifically in the intestine of intestine-specific *Rab11a* knockout (IKO) mice (*Villin-Cre; Rab11a*$^{flox/flox}$) by Western blot analysis (Fig. 5A). The IKO mice were born with smaller body

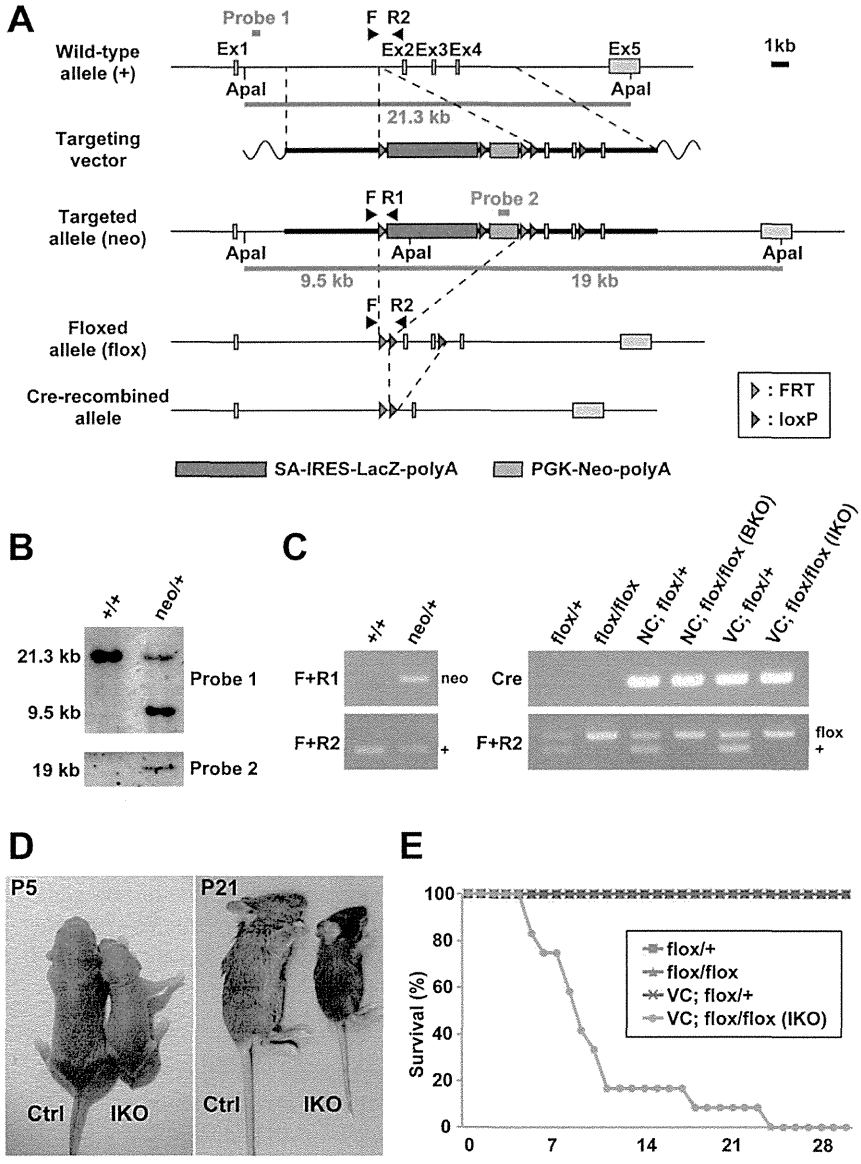

Fig. 1. Generation and analysis of *Rab11a* knockout mice. (A) Diagram of targeting strategies. Restriction maps of the *Rab11a* wild-type allele (+), the targeting vector containing an SA-IRES-LacZ-polyA sequence (blue horizontal bar) and PGK-Neo-polyA (orange horizontal bar), and the targeted allele (neo). Brown triangle, loxP site; green triangle, FRT site. Probe 1 hybridises with a 21.3-kb Apa I fragment from the wild-type allele and a 9.5-kb fragment from the targeted allele. Probe 2, the neomycin fragment in PGK-Neo-polyA, hybridises with a 19-kb Apa I fragment from the targeted allele. SA, splice acceptor; IRES, internal ribosomal entry site; PGK, phosphoglycerate kinase promoter; Neo, neomycin resistance gene cassette. (B) Southern blotting analysis of the targeted ES cell clones. Genomic DNA from parental embryonic stem cells (+/+) and targeted clones (neo/+) were digested with Apa I for hybridisation with the probes 1 and 2 in (A). (C) Genotyping PCR analysis using genomic DNA from control and knockout mouse tails. Primers 'F+R1', primers 'F+R2', and primers 'Cre' were used to detect the targeted allele (neo), the wild-type (+) and floxed (flox) alleles, and *cre* gene. (D) Control (Ctrl) and intestine-specific *Rab11a* knockout (IKO) mice at postnatal days 5 (P5) and 21 (P21). The IKO mice were smaller than control littermates at both ages. (E) Survival curves for control (n=12–14) and IKO (n=12) mice. IKO mice began dying 5 days after birth, and all mice were dead by postnatal day 25. NC, *Nestin-Cre*; VC, *Villin-Cre*.

Biology Open (2015) 000, 1–9 doi:10.1242/bio.20148532

size than controls and most died within 2 weeks after birth (Fig. 1D,E and supplementary material Table S1). When we examined the distribution of apical and basolateral proteins in the IKO mice by immunofluorescence, we found mislocalisation of apical proteins in intestinal epithelial cells (Figs 2, 3). The apical protein dipeptidyl-peptidase 4 (DPPIV) distributed in the cytoplasm and colocalised with the lysosome marker lysosomal-associated membrane protein 2 (Lamp2) at P5 and P21 (Fig. 2, arrows). In addition, DPPIV was found to be mislocalised to the basolateral plasma membrane, which was evident in the epithelial cells at P5 (Fig. 2B, arrowheads). Accumulated DPPIV did not colocalise with the trans-Golgi network (TGN) marker Golgin97 (Fig. 3A). Other apical proteins, such as alkaline phosphatase (AlP) and aminopeptidase N (APN), were also found to accumulate within the cytoplasm (arrowheads) and mislocalised to the basolateral plasma membrane (arrows) in the IKO mice (Fig. 3B). In contrast, no basolateral proteins were mislocalised at P5 and P21 (Fig. 3C).

The accumulation of apical proteins was previously observed in *Rab8a* knockout mice and *Rab8a/Rab8b* double-knockout mice (Sato et al., 2007; Sato et al., 2014). Since we also reported a shortening of microvilli and microvillus inclusion bodies in these mice, we observed these phenotypes in the small intestine of *Rab11a* IKO mice using electron and light microscopy (Fig. 4). Next, we analysed the terminal web, which is an actin-based filamentous structure associated with microvilli. Though the terminal web was stained by alpha-actinin (Geiger et al., 1979), there was no obvious difference in the width of this structure between the control and *Rab11a* IKO mouse (supplementary material Fig. S4A,B). This result indicates that the terminal web was not significantly affected in *Rab11a* IKO.

Decreased apical protein levels in the small intestine of *Rab11a* IKO mice cause starvation

When we assessed the levels of apical and basolateral proteins in the small intestine by western blot, the levels of apical proteins (DPPIV and AlP) were lower in the IKO mice than those in the control mice. In addition, the molecular weights of DPPIV and AlP of the IKO mice appeared higher than those of the control mice (Fig. 5A). As we postulated that the apparent higher molecular weights were due to abnormal glycosylation, we treated DPPIV with peptide *N*-glycosidase (PNGase F) to remove *N*-linked carbohydrates. After PNGase F treatment, the molecular weight of DPPIV of IKO became similar to that of control (Fig. 5B), indicating there is no significant difference in the molecular weight of non-glycosylated protein between IKO and control. In contrast, the localisation of basolateral proteins appear intact (Fig. 3C). However, the amount of Na^+K^+-ATPase, one of basolateral proteins, was increased in the IKO than that in the control (Fig. 5A). However, the amount of other basolateral markers (LDL-R and E-cadherin) were not changed. Thus, the loss of Rab11a affects the amount of some basolateral protein (Na^+K^+-ATPase). As the Rab11a IKO mice were runted and died at early postnatal period like *Rab8a* KO mice (Sato et al., 2007), we examined whether IKO mice were also starved to death. We observed an increase in the level of a starvation marker (total ketone bodies) in the blood of the IKO mice (Fig. 5C). These data suggest that similar molecular mechanisms are responsible for lethality in the *Rab11a* IKO mice and *Rab8a* KO mice (Sato et al., 2007). Namely, the mislocalisation of apical proteins (e.g., enzymes and transporters) in these knockout mice may lead to decreased nutrient uptake, causing starvation and death.

Rab11a functionally interacts with Rab8a and myosin Vb *in vivo*

As the phenotypes of *Rab11a* IKO mice were similar to those of *Rab8a* knockout mice, we thought that Rab11a and Rab8a might function in cooperation for apical transport pathway to some extent. We then examined the localisation of Rab8a in the epithelial cells of the IKO mice and *vice versa*. Indeed, we found that Rab8a was mislocalised in the IKO mice and that Rab11a was mislocalised in *Rab8a* knockout mice compared with control

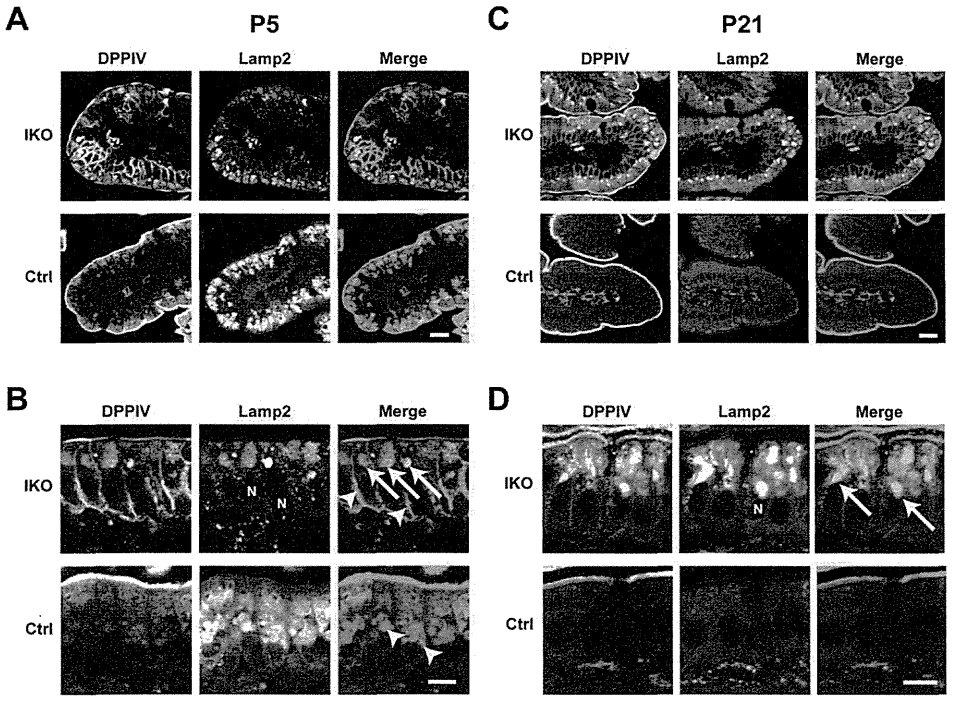

Fig. 2. Localisation of the apical protein DPPIV in the small intestine of *Rab11a* IKO mice at P5 and P21. (A–D) Localisation of the apical protein DPPIV (green) and the lysosome marker Lamp2 (red) in control (Ctrl) and IKO mice at P5 (A,B) and P21 (C,D). Higher magnification views of the intestinal cells from Ctrl and IKO mice at P5 (B) and P21 (D). At P5 (A,B), intracellular DPPIV staining (green) is colocalised with Lamp2 (red) in IKO cells (arrows in B 'IKO'), whereas DPPIV and Lamp2 (arrowheads in B 'Ctrl') did not colocalise in control cells. In addition, basolateral staining (arrowheads in B 'IKO') is more evident in IKO cells. At P21 (C,D), intracellular DPPIV staining is evident and the colocalisation of Lamp2 and DPPIV is greater in IKO mice (arrows in D). Scale bars: 20 μm (A,C), 10 μm (B,D).

Biology Open (2015) 000, 1–9 doi:10.1242/bio.20148532

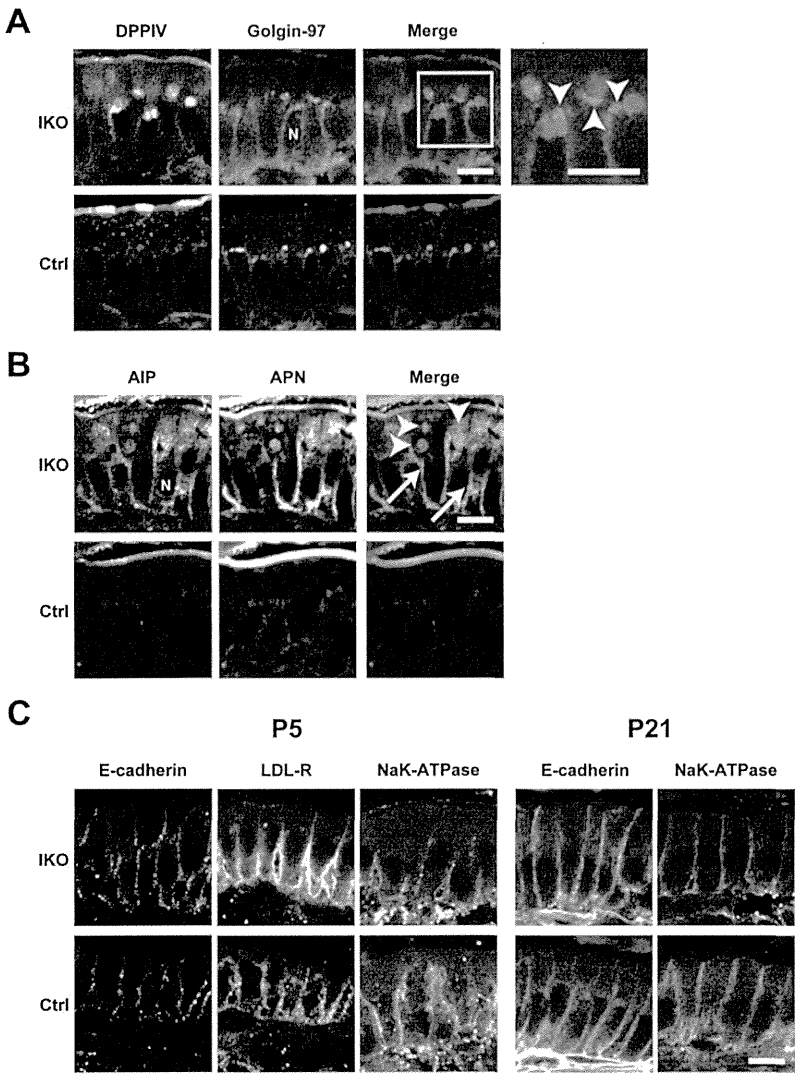

Fig. 3. Localisation of apical and basolateral proteins in the small intestine of *Rab11a* IKO mice at P21. (A) DPPIV and the TGN marker Golgin-97 (arrowheads) do not colocalise in intestinal epithelial cells from IKO mice at P21. High-magnification insets (white boxes) are shown to the right of these panels. (B) Localisation of the apical proteins AIP and APN in control (Ctrl) and IKO cells at P21. Merged figures of AIP and APN are shown on the right. Intracellular vacuoles of AIP and APN are indicated by arrowheads. Basolateral localisation is indicated by arrows. (C) Localisation of the basolateral proteins E-cadherin, Na^+K^+-ATPase, and LDL-R in epithelial cells of the small intestine in Ctrl and IKO mice is not different at P5 and P21. Scale bars: 10 μm. N, nucleus.

mice, demonstrating a functional relationship between these proteins (Fig. 6A,B). Both Rab8a and Rab11a are known to bind myosin Vb (Lapierre et al., 2001; Roland et al., 2007; Jin et al., 2011). Therefore, to determine whether myosin Vb protein is involved in the localisation of Rab11a, we compared small intestine samples from a microvillus atrophy patient and a healthy individual (Fig. 6C), as microvillus atrophy patients are known to have mutations in the *myosin Vb* gene (Müller et al., 2008). In the healthy small intestine, Rab11a localised subapically (Fig. 6C). However, in the small intestine of the microvillus atrophy patient, Rab11a localised closer to the nucleus (Fig. 6C). Taken together, these results indicate that Rab11a appears to functionally interact with Rab8a and myosin Vb *in vivo*.

Rab11a is important for apical transport in the intestine during early postnatal period

Although the phenotypes of *Rab11a* IKO mice and *Rab8a* knockout mice were similar, the onset of the phenotype was earlier in the IKO mice (begin dying from 5 days after birth) than in the *Rab8a* knockout mice (begin dying from 3 weeks after birth) or *Rab8a/8b* double-knockout mice (begin dying from 2 weeks after birth). To investigate these differences, we performed Western blot and immunofluorescence analyses on wild-type small intestines during postnatal development. As determined by immunofluorescence, Rab11a primarily localises to the subapical region from birth until 10 days after birth (Fig. 7A). In contrast, Rab8a primarily localises to the perinuclear region and is nearly absent by P21, as previously described (Sato et al., 2007) (Fig. 7A). These data suggests that Rab11a and Rab8a might function during different steps of the apical transport process in the epithelial cells. As determined by Western blot analysis, Rab8a protein levels increased over the first 10 days after birth and then gradually faded, as previously described (Sato et al., 2007) (Fig. 7B). In contrast, Rab10 was consistently expressed throughout postnatal development, although the levels moderately increased 3 weeks after birth (Fig. 7B). Rab11a was abundantly expressed until 2 weeks after birth (Fig. 7B). These data demonstrate that the IKO mice die during the period when Rab11a levels are normally most abundant, suggesting the importance of this protein in apical transport in the small intestine during the early postnatal period.

DISCUSSION

In this study, we generated conventional (systemic), brain-specific, and intestine-specific *Rab11a* knockout mice. The conventional knockout mice were embryonic lethal

Biology Open (2015) 000, 1–9 doi:10.1242/bio.20148532

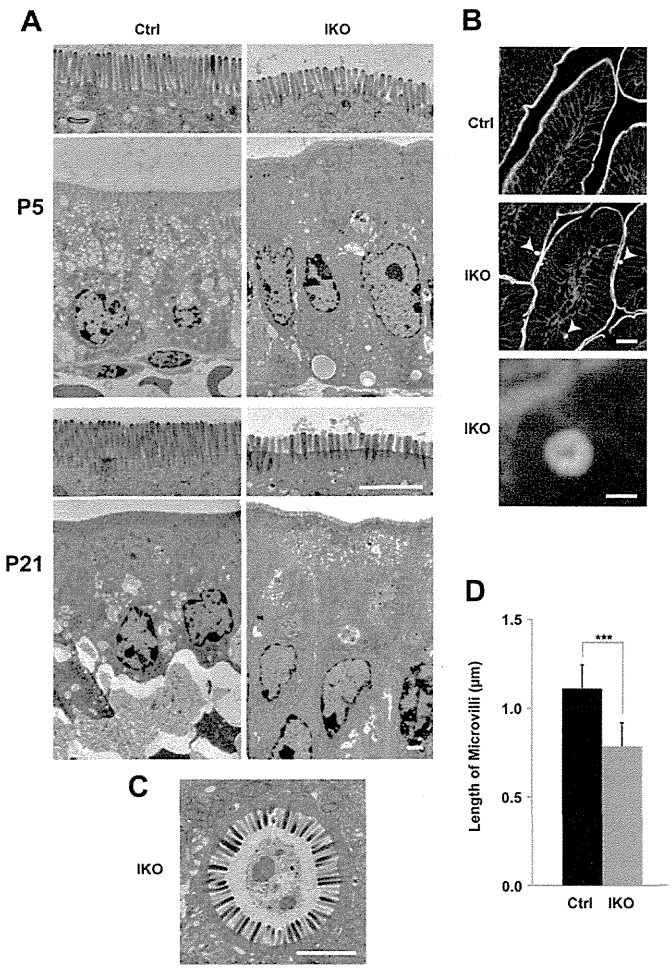

Fig. 4. Microvillus atrophy and inclusions in *Rab11a* IKO mice.
(A) Electron micrographs of P5 and P21 intestinal cells. Apical microvilli (first and third panels from top) are shorter in knockout cells (IKO) than in control (Ctrl) cells. (B) Sections of intestinal cells at P21 stained with phalloidin. F-actin localisation is prominent in the apical plasma membranes in villi of control intestines (top panel). Phalloidin-positive intracellular spheroids are evident in mutant villi (arrowheads in the middle panel). An enlarged view is shown in the bottom panel. (C) A microvillus inclusion body from a P21 IKO intestinal epithelial cell visualised using electron microscopy. (D) A graph showing microvillus length in epithelial cells at P5. Values represent mean ± s.d. (n>40 cells randomly selected from three mice per group; *** $P<0.001$; Student's *t*-test). Scale bars: 2 μm (A,C), 20 μm (B, middle), 2 μm (B, bottom).

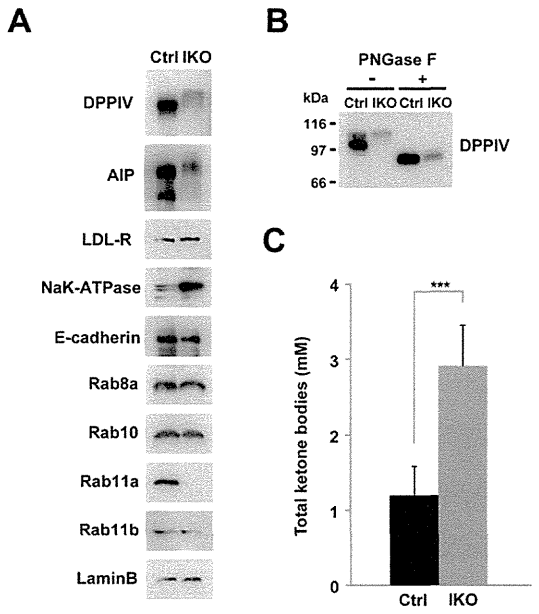

Fig. 5. Quantification of a starvation marker and protein levels.
(A) Western blot analysis of protein levels in crude extracts from the small intestines of control (Ctrl) and IKO mice at P5. Small intestine extracts were analysed by Western blot analysis using antibodies against various apical proteins (DPPIV and AIP), basolateral proteins (LDL-R, Na^+K^+ATPase, and E-cadherin), Rabs (Rab8a, 10, 11a, and 11b), and a loading control (Lamin B). (B) Treatment of peptide *N*-glycosidase F (PNGase F) in lysates from the small intestine of control (Ctrl) and IKO mice at P5. The samples were analysed by Western blotting using anti-DPPIV antibody. (C) Amounts of total ketone bodies in control (Ctrl) and IKO mice at P5. Values represent means ± s.d. from 4–10 mice. ***$P<0.001$; Student's *t*-test.

(supplementary material Table S1). The brain-specific knockout mice displayed no overt phenotypes (supplementary material Figs S1–S3). However, we found that Rab11a is essential for the proper localisation of apical proteins in the intestine (Figs 2, 3). Rab11 is known to localise to apical recycling endosomes in polarised cells (Casanova et al., 1999), and it has been reported that Rab11 is involved in shuttling membranes from intracellular vesicles to the plasma membrane in a variety of organisms (yeast, fly, worm, and mouse) (Benli et al., 1996; Li et al., 2007; Sato et al., 2008; Duman et al., 1999; Khandelwal et al., 2008; Khandelwal et al., 2013). Recently, it was shown that recycling endosomes are essential for biosynthetic transport from the TGN to plasma membrane by functionally disrupting recycling endosomes (Ang et al., 2004). Cresawn et al. also showed that apical recycling endosomes are an essential route for the biosynthetic transport of 'raft'-associated apical cargos to the apical plasma membrane from the TGN (Cresawn et al., 2007). These reports suggest the involvement of Rab11 in the apical transport of several proteins through a number of biosynthetic pathways. Here, we showed that the loss of Rab11 leads to the mislocalisation of apical proteins in the small intestine using *Rab11a* IKO mice (Figs 2, 3). Furthermore, as we detected abnormal *N*-glycosylation of apical proteins in *Rab11a* IKO mice (Fig. 5A,B), Rab11a is likely to be involved in apical biosynthetic transport in small intestinal epithelial cells. We presume that depletion of Rab11a decelerates apical protein transport through the Golgi apparatus and increases *N*-glycosylation of apical proteins. We should perform more experiments in future to test this idea.

Rab11 proteins have a number of binding partners, including myosin Vb (Lapierre et al., 2001; Hales et al., 2001), which is also known to bind Rab8 and Rab10 (Roland et al., 2007; Roland et al., 2009). The human *myosin Vb* gene is mutated in microvillus inclusion disease, which is characterised by the mislocalisation of apical proteins, shortening of microvilli and microvillus inclusion bodies. These phenotypes are also observed in *Rab8a* knockout mice and *Rab8a/Rab8b* double-knockout mice (Sato et al., 2007; Sato et al., 2014; Müller et al., 2008), suggesting a close functional relationship between myosin Vb and Rab8. Here, we observed shorter microvilli and microvillus inclusion bodies in *Rab11a* IKO mice (Fig. 4) and showed that Rab11a and Rab8a depend on one another for proper localisation (Fig. 6A,B). We also observed that the localisation of Rab11a in the small intestinal tissue from a microvillus atrophy patient was

Biology Open (2015) 000, 1–9 doi:10.1242/bio.20148532

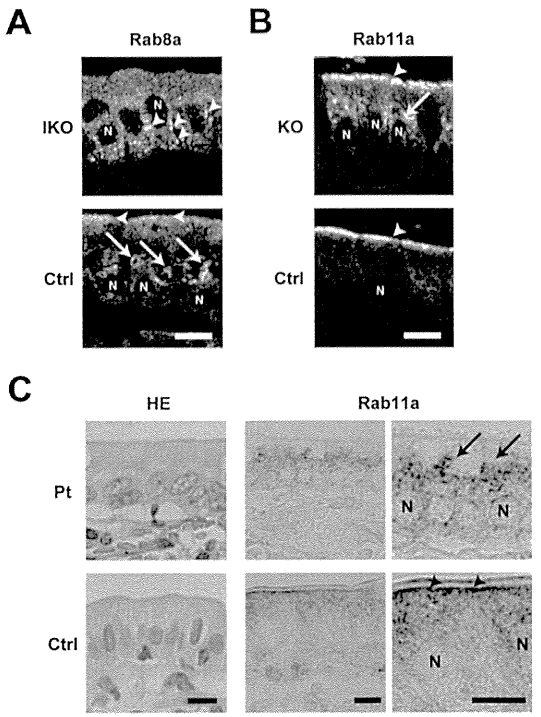

Fig. 6. Spatial interdependence between Rab11a, Rab8a, and myosin Vb. (A) Localisation of Rab8a in epithelial cells of the small intestine in control (Ctrl) and *Rab11a* IKO mice at P5. Rab8a is mainly localised on perinuclear punctate structures (arrowheads) below the nucleus (N) in IKO cells, whereas it is localised on large vacuolar structures (arrows) above the nucleus in control cells. (B) Localisation of Rab11a in epithelial cells of the small intestine in Ctrl and *Rab8a* KO mice at P7. Rab11a is exclusively localised below the apical plasma membrane (an arrowhead) in Ctrl epithelial cells, but it is also localised punctate structures (an arrow) above the nucleus in *Rab8a* KO epithelial cells. (C) Localisation of Rab11a in epithelial cells of the small intestine from a control (Ctrl) and a microvillus atrophy patient (Pt). Rab11a is localised below the apical plasma membrane in control intestinal cells (arrowheads), but it is localised perinuclear structures in patient's intestinal cells (arrows). HE Scale bars: 10 μm. N, nucleus.

different from that in a healthy intestinal tissue (Fig. 6C). These results indicated that the localisation of Rab11a, Rab8a, and Myosin Vb were dependent on one another, suggesting the functional relationship between these proteins. Notably, the localisation of Rab11a was obviously different from that of Rab8a (Fig. 7A). It is likely that Rab11a and Rab8a regulate different steps of the same apical transport pathway by utilizing the common binding protein, Myosin Vb. This is similar to the case in yeast. Myo2p which is a homolog of mammalian Myosin Vb sequentially associates with Ypt31p and Sec4p, homologs of Rab11a and Rab8a respectively (Santiago-Tirado et al., 2011; Mizuno-Yamasaki et al., 2010).

Rab11a IKO mice displayed a similar phenotype, such as mislocalisation of apical proteins, shortening of microvilli, and microvillus inclusion body formation, to those of *Rab8a* knockout and *Rab8a/Rab8b* double-knockout mice (Figs 2–4). However, the phenotype in the IKO mice was apparently much earlier than in *Rab8a/Rab8b* double-knockout mice. Therefore, Rab11a appears to be a key molecule in apical transport, even when Rab8a plays minor roles for it. Furthermore, at a later postnatal period (P21) when Rab8a is required, *Rab11a* IKO mice show a very similar phenotype to Rab8a KO mice. Based on these results, we conclude that Rab11a is essential for apical transport independently of Rab8, and indeed, Rab11a appears to play an even more critical role in this process than Rab8 (Fig. 7).

Finally, *Rab11a* BKO mice appeared normal and displayed no obvious abnormalities (supplementary material Figs S1–S3). Previous studies have reported that Rab11 is essential for neurite elongation through a number of effectors (Shirane and Nakayama, 2006; Takano et al., 2012). However, compensation by other Rab11 family proteins, particularly Rab11b, cannot be ruled out, as mice deficient for another Rab11 family protein, Rab25, displayed no overt neuronal phenotype. Regardless, we found this result surprising due to the variety of localisations and roles proposed for each Rab11 family (Lapierre et al., 2003). To more fully characterise the role of Rab11 family members in the nervous system, it will be necessary to examine brain-specific *Rab11a* knockout mice in greater detail, as well as to generate *Rab11b* knockout mice and/or brain-specific *Rab11a*, *Rab11b*, and *Rab25* double- or triple-knockout mice.

MATERIALS AND METHODS

Generation of *Rab11a* knockout mice

All animal procedures were performed according to the guidelines of the Animal Care and Experimentation Committee of Osaka University, and all animals were bred at the Institute of Animal Experimental Research of Osaka University.

Rab11a knockout mice were generated largely as described previously (Harada et al., 1994). *Rab11a* knockout ES clones (*Rab11a*$^{tm1a(KOMP)Wtsi}$) were provided by the UC Davis KOMP Repository.

Targeted clones were confirmed by Southern blotting analysis (Fig. 1B) prior to blastocyst injection. To generate *Rab11a*$^{flox/+}$mice, we crossed *Rab11a*$^{neo/+}$ mice with actin-flippase transgenic mice (B6; SJL-Tg (ACTFLPe) 9250 Dym/J) (Jackson Laboratory, Bar Harbor, ME, USA). To generate brain-specific and intestine-specific *Rab11a*-knockout mice, we crossed *Rab11a*$^{flox/+}$ mice with *Nestin-Cre* transgenic mice (Tronche et al., 1999) and *Villin-Cre* transgenic mice (Madison et al., 2002) (Jackson Laboratory, Bar Harbor, ME, USA), respectively.

Genotypes in animals were confirmed by PCR using genomic DNA from tails of control and knockout mice. Primers used for genotyping PCR were as follows: primer 'F', 5′-TAA GCC TCG TGC CTC CTG TTT TAA-3′; primer 'R1', 5′-ACC TTG GGC AAG AAC ATA AAG TGA-3′; primer 'R2', 5′-ATT CCT ATT TAG GAA CTC ACA CCC-3′; primers 'Cre', 5′-AGG TTC GTT CTC TCA TGG A-3′ (*cre* forward); 5′-TCG ACC AGT TTA GTT ACC C-3′ (*cre* reverse).

Immunofluorescence and immunoblotting

Mice at different postnatal days were anesthetised and fixed by intracardial perfusion or immersion with 3% paraformaldehyde in 0.1 M phosphate buffer (pH 7.2) and further fixed for 2 h in the same fixative. For cryoprotection, the fixed tissues were soaked in a series of 4, 10, 15, and 20% sucrose in 0.1 M phosphate buffer (pH 7.2) at 4°C for at least 30 min for each step. The tissues were then frozen in isopentane chilled in liquid nitrogen and stored in liquid nitrogen until cryosectioning. The tissues were cut into 5–10 μm sections. Western blotting (WB) was performed as previously described (Sato et al., 2011) with 10 μg of protein per lane.

The following antibodies and dyes were used in this study (dilutions refer to immunofluorescence (IF) assays, unless otherwise noted): actinin-4 (1:100; Alexis biochemicals, San Diego, CA, USA); AIP (1:1000 for WB, 1:100 for IF; Rockland, Gilbertsville, PA, USA); APN (1:100; BMA Biomedicals, Augst, Switzerland); Arl13b (1:1000; ab136648; Abcam, Cambridge, MA, USA); calbindin (1:100; Santa Cruz Biotechnology, Dallas, TX, USA); Cux1 (1:50; Santa Cruz Biotechnology, Dallas, TX, USA); dipeptidyl-peptidase 4 (DPPIV; 1:100; R&D Systems, Minneapolis, MN, USA); 4′,6-Diamidine-2′-phenylindole dihydrochloride (DAPI; 1:1000; Roche, Basel, Switzerland); E-cadherin (1:1000 for WB; BD, San Jose, CA, USA, 1:50 for IF; TAKARA, Shiga, Japan); GAPDH (1:2000 for WB; EMD